APPENDIX 14

MET OCEAN ASSESSMENT REPORTS

Appendix 14 includes:

- Appendix 14A: Hydrodynamic Assessment;
- Appendix 14B: Morphodynamic Assessment;
- Appendix 14C: Dredge Plume Modelling Assessment;
- Appendix 14D: Pipi Larvae Modelling Assessment;

APPENDIX 14A

HYDRODYNAMIC ASSESSMENT

MINISTRY OF BUSINESS, INNOVATION & EMPLOYMENT
HĪKINA WHAKATUTUKI

New Zealand Government
Te Kāwanatanga o Aotearoa

Hydrodynamic Modelling MBIE 2026 Update

Effects of Proposed Reclamation and Dredging Layout on Hydrodynamics

(Design July 2026)

Report prepared for MBIE

August 2026

MetOcean SOLUTIONS

Document History

Versions

Version	Revision Date	Summary	Reviewed by
0.1	20/07/2026	Draft for client review	Watson/Berthot/Beamsley
0.1	07/08/2026	Draft for internal review	Beamsley

Distribution

Version	Date	Distribution
1.0	07/08/2026	FINAL - MBIE project team

Document ID: P0678 - 06

Authors

Berthot A., Watson H., B Beamsley.

Contributors

Carle E.,

Disclaimer:

This document has been prepared by Meteorological Service of New Zealand Limited (MetService) under contract to the Ministry of Business, Innovation and Employment (MBIE) for and in relation to the Northland Dry Dock project, including, without limitation, the consent application (Purpose) and in accordance with the Code of Conduct for Expert Witnesses contained in the Environment Court Practice Note 2023. This document may include numerical modelling undertaken in accordance with good industry practice, using appropriate methodologies, data, and assumptions, and prepared with due care, skill, and diligence consistent with the standards required and expected of a leading supplier in the relevant field ("Data Modelling Best Practice"). MetService accepts no responsibility on any ground for any loss, damage or expense arising from:

- any use of or reliance on this document or any part of it by any person who is not authorised by MetService or MBIE to use it for the Purpose;
- any use of or reliance on this document or any part of it by any person outside the Purpose;
uncertainty in numerical modelling, to the extent that such uncertainty could not reasonably have been avoided, reduced, managed or mitigated through Data Modelling Best Practice.

Contents

List of Figures

List of Tables

1. Introduction

Northport is a deep-water commercial port strategically situated at Marsden Point near Whangarei in Northland, New Zealand (Figure 1-1).

The Ministry of Business, Innovation and Employment (MBIE) seeks approvals pursuant to the Fast-track Approvals Act 2024 for a shipyard and drydock facility (Northland Shipyard and Drydock Facility, NSDF) abutting the western side of the existing Northport facility at Marsden Point (Figure 1-*2*). The project includes a reclamation, vessel haul-out system, and associated wharf structures, dredging and supporting infrastructure.

Key components of the project include:

- Reclamation of approximately 9.5 hectares
- A 'cutout' to the reclamation where a vessel haul out system is to be located, being a floating drydock or potentially shiplift or other lifting mechanism,
- Construction of a piled wharf structure to accommodate vessels either temporarily (before/after haul-out), or for extended periods where works not requiring haul out can be undertaken,
- Capital and maintenance dredging associated with construction and ongoing operation of the marine maintenance operations facility, including a berth pocket and a vessel turning basin to provide for safe navigation,
- Fixed plant and buildings to accommodate marine maintenance activities and materials,
- Sufficient working and laydown areas for marine maintenance operations, including the ability to transfer vessels to hardstand,
- Access to and around the marine maintenance operations facility, including a landside area for staff carparking,
- Public access around the edge of the reclamation to a public fishing platform.

MetOcean Solutions (MOS, a division of the Meteorological Service of New Zealand) has undertaken a number of numerical hydrodynamic and morphological modelling simulations and dredged plume dispersion simulations related to operations and expansion of Northport, with results presented in MOS reports P0367-01 to P0367-06 (MetOcean Solutions, 2018a, 2018b, 2018c, 2018d, 2018e, 2018f), in 2021 reports P0519-01 to P0519-03 (MetOcean Solutions, 2021a, 2021b, 2021c) and in 2022 reports P0519-10 to P0519-13 (MetOcean Solutions, 2023, 2022a, 2022b).

This technical report provides the outcomes of hydrodynamic modelling for three proposed scenarios:

1. The existing environment
2. The proposed shipyard and drydock facility (Design West, Figure 2-1); and
3. The proposed shipyard and drydock facility AND the recently consented Eastern Reclamation (Design East and West, Figure 2-2).

The hydrodynamic modelling included the following tasks:

- Review grid spacing in the area around the proposed reclamation and dredge footprints, including refining the hydrodynamic grid to ensure structures and batter slopes are accurately captured within the numerical model.
- Simulations of hydrodynamic with the two designs and comparison to simulations with the existing bathymetry (updated with the latest 2026 survey). Runs over a full month of hydrodynamic (2 spring/neap cycles) modelling and an assessment of change in currents over a typical spring and neap tidal cycle.

The structure of this report is as follows:

- Section 2 presents a summary of previous study undertaken at the site and the datasets used in the study.
- Section 3 describes the methodology and model setup.
- In Section 4, results of hydrodynamic modelling from both Existing and the two proposed bathymetry layouts are presented.
- Section 5 provides a summary of this report.
- Section 6 includes a list of references.

Figure 1-1 Location of Northport within Whangarei Harbour.

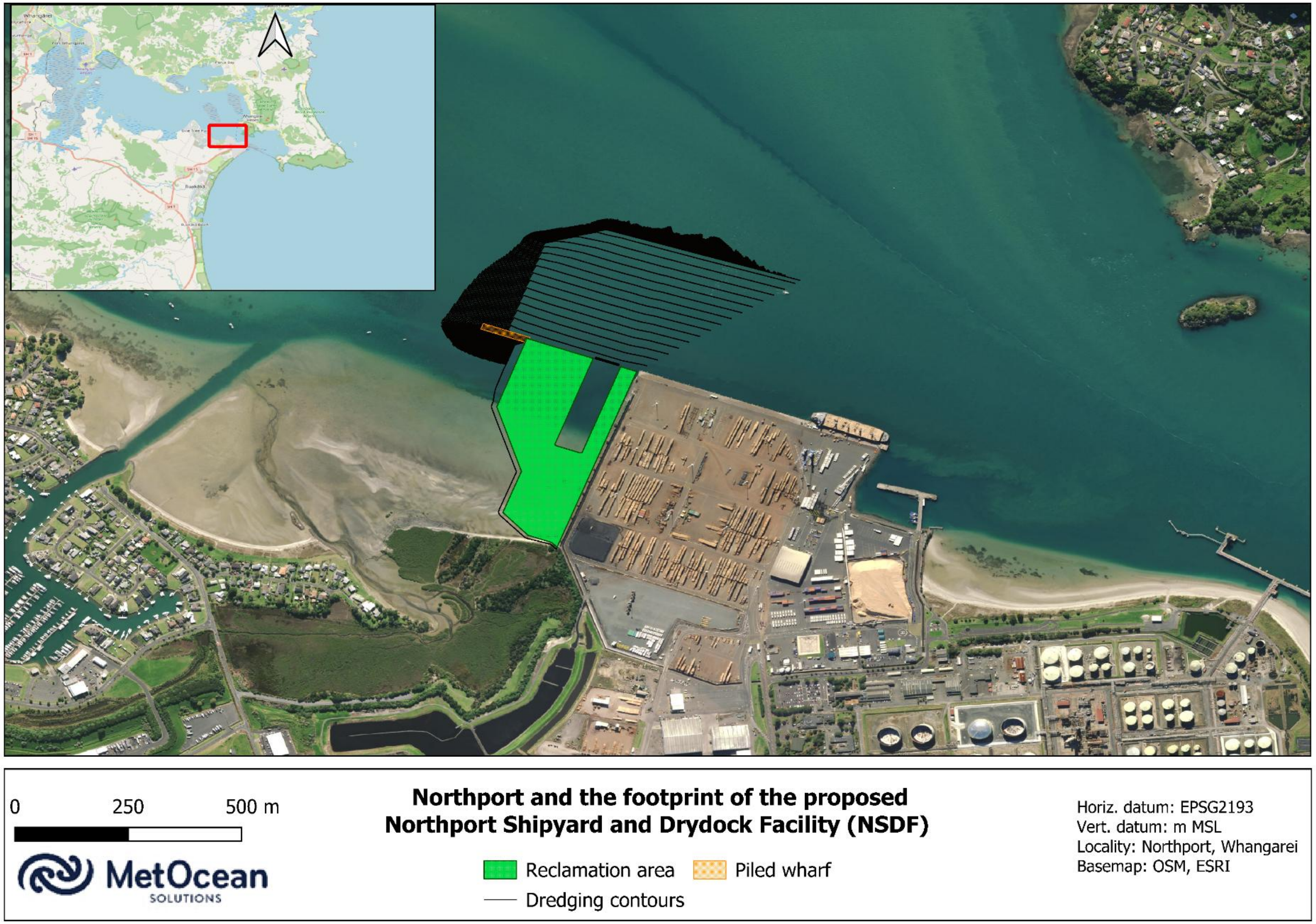

Figure 1-2 Proposed Northland Shipyard and Drydock Facility (NSDF) adjacent to Northport, Whangarei.

2. Data

2.1 Previous studies

Over the last 15 years, MetOcean Solutions has undertaken several modelling studies of the Whangārei Harbour. The characterisation of the physical environment of the Whangārei Harbour and the establishment of wave, current and sediment dynamics numerical models initiated in 2015-2016 with the (then) Refining New Zealand (RNZ) proposed deepening of the shipping channel to the (then) Marsden Point Refinery (MetOcean Solutions, 2016).

Each of the model software used in the studies was selected for a specific technical requirement. The numerical models included:

- SWAN[1] (Simulating Waves Nearshore) wave model (Holthuijsen et al., 2007)
- ROMS hydrodynamic model, (Regional Ocean Modelling System, described in (Haidvogel, D.B et al., 2008))
- SELFE/SCHISM hydrodynamic model (Zhang and Baptista, 2008)
- Delft3D Hydrodynamic/Wave/Sediment Transport suite (Deltares, 2018a, 2018b).
- ERcore Lagrangian particle tracking model.

The work presented in this report was built upon the existing knowledge and previous model setups and development. An overview of the work previously undertaken using the SCHISM model are:

- The models were calibrated and validated with available measured data. Details and examples of the model validation can be found in previous reports (MetOcean Solutions, 2021a, 2018f).
- Effects of proposed reclamation layouts on hydrodynamics using the calibrated and validated SCHISM model was undertaken for three scenarios, Full Vision for Growth scenario[2] (VFG), original Northport Western Shipyard only (which differs from the currently proposed design), Eastern reclamation only. The outcomes and configurations were presented in MOS report P0519-01 (MetOcean Solutions, 2021a).

---

[1] Modified from SWAN version of the 40.91 release (publicly available code)

[2] The Northport Vision for Growth project was a Resource Consent project formally granted on **2 October 2025**, completing the consent process

- An evaluation of sensitivity to wind driven currents was also undertaken. The outcome was that wind-driven currents are not significant within the proposed dredging and reclamation regions, and tidal current are expected to dominate there. However, the wind field can trigger additional current speed of 0.3 $m.s^{-1}$ in shallow areas of the harbour and along the port entrance. Therefore, it was recommended that the atmospheric forcing is included in the SCHISM model and they were included in the 2021 study.
- Results from the 2021 study found that changes in the current field were confined to the region where the dredging and reclamation works would be undertaken and changes in current speed during a spring tide were expected to be typically less than 0.1 $m.s^{-1}$. There was also a small decrease in predicted currents near the Western and Eastern reclamation ends, associated with swinging basin deepening, which indicated a potential for increased sedimentation in this area.
- In 2022 the model mesh was further developed and refined over the port area to better represent the proposed designs. The hydrodynamics of the area were evaluated against Existing bathymetry for one layout, which was the Eastern Reclamation, results were presented in MOS report P0519-10 (MetOcean Solutions, 2022a).
- Results from the 2022 modelling showed that changes in the current field are confined to the region where the dredging and reclamation works were to be undertaken. A small decrease in currents near the eastern end of the Eastern Reclamation area indicated a potential for increased sedimentation. The western edge of the dredge footprint is also expected be subject to an increase in sedimentation.

2.2 Scenarios

Besides the existing harbour configuration, there are two proposed scenarios that have been modelled:

- **Design West** includes the Northland Drydock and Shipyard Facility (NDSF) proposed by MBIE (Figure 2-1), and
- **Design East and West** includes the Northland Drydock and Shipyard Facility proposed by MBIE and Northport's consented Eastern Development (reclamation and dredging) (Figure 2-2),

The three naming conventions of Existing, Design West, Design East and West are used within the simulations.

Figure 2-1 Concept drawing for the proposed area to be dredged and reclaimed for Design West.

Figure 2-2 Concept drawing for the proposed area to be dredged and reclaimed for Design East and West.

2.3 Bathymetry datasets

Bathymetry is an important input of numerical models. In this study, provided, open source, and archival bathymetry and topographic data covering and surrounding areas were identified and selected for inclusion in the bathymetry grid as summarised in Table 2-1.

The previous bathymetry dataset used was updated with the latest bathymetry and topographic survey data from Table 2-1, as shown in Figure 2-3. The NDSF and eastern reclamation designs were provided by MBIE, with the designs incorporated into the existing bathymetry (Figure 2-5 to Figure 2-6).

Table 2-1 Summary of bathymetry and topographic data used for the model bathymetry.

Name	Coverage Area	Data Type	Data Acquisition Method(s)	Resolution	Vertical Datum	Source
2026 Port MBES Survey	Whangārei Harbour Channel, Marsden Bay Channel, Mair Bank Transects	Bathymetry	Multibeam Echosounder	50 cm	CD (Marsden Point)	DML Survey provided by Northport
2026 Port SBES Survey	Mair Bank and Marsden Point	Bathymetry	Singlebeam Echosounder	1 m point spacing	CD (Marsden Point)	DML Survey provided by Northport
2025 Snake Bank SBES Survey	Eastern Snake Bank	Bathymetry	Singlebeam Echosounder	20 m transects with 1 m point spacing	CD (Marsden Point)	DML Survey provided by Northport
2025 Marsden Bay SBES Survey	Nearshore areas of Marsden Bay	Bathymetry	Singlebeam Echosounder	40 m transects with 50 cm point spacing	CD (Marsden Point)	DML Survey provided by Northport
2025 Marsden Bay MBES Survey	Marsden Bay Channel and western area of Marsden Bay	Bathymetry	Multibeam Echosounder	50 cm	CD (Marsden Point)	DML Survey provided by Northport
2025 Northport MBES Survey	Northport dredging basin and proposed dredging/reclamation areas	Bathymetry	Multibeam Echosounder	50 cm	CD (Marsden Point)	DML Survey provided by Northport
2024 Ruakaka SBES Survey	Ruakaka transects	Bathymetry	Singlebeam Echosounder	20 m point spacing	NZVD	MetOcean Archive

2024 Bream Bay MBES Survey	17 km2 area in Bream Bay	Bathymetry	Multibeam Echosounder	1 m	NZVD	MetOcean Archive
2024 Portland Channel MBES Survey	Portland Channel	Bathymetry	Multibeam Echosounder	50 cm	CD (Marsden Point)	DML Survey provided by Northport
2024 Northland Lidar	Coastal areas to 0.3 m below MSL	Topography	Lidar	1 m	NZVD	LINZ Data Service
2023 Whangārei Harbour Channel MBES Survey	Whangārei Harbour Channel	Bathymetry	Multibeam Echosounder	1 m	CD (Marsden Point)	DML Survey provided by Northport
2022 MetOcean Northport Model Bathymetry	Whangarei Harbour, Northport, and Bream Bay	Bathymetry	Various	Various	MSL	MetOcean Archive
1999 Shipping Lane 1 MBES	Bream Bay shipping lane	Bathymetry	Multibeam sonar	20 m	LAT	LINZ Data Service
2026 Port MBES Survey	Whangārei Harbour Channel, Marsden Bay Channel, Mair Bank Transects	Bathymetry	Multibeam Echosounder	50 cm	CD (Marsden Point)	DML Survey provided by Northport
2026 Port SBES Survey	Mair Bank and Marsden Point	Bathymetry	Singlebeam Echosounder	1 m point spacing	CD (Marsden Point)	DML Survey provided by Northport
2025 Snake Bank SBES Survey	Eastern Snake Bank	Bathymetry	Singlebeam Echosounder	20 m transects with 1 m point spacing	CD (Marsden Point)	DML Survey provided by Northport

2025 Marsden Bay SBES Survey	Nearshore areas of Marsden Bay	Bathymetry	Singlebeam Echosounder	40 m transects with 50 cm point spacing	CD (Marsden Point)	DML Survey provided by Northport
2025 Marsden Bay MBES Survey	Marsden Bay Channel and western area of Marsden Bay	Bathymetry	Multibeam Echosounder	50 cm	CD (Marsden Point)	DML Survey provided by Northport
2025 Northport MBES Survey	Northport dredging basin and proposed dredging/reclamation areas	Bathymetry	Multibeam Echosounder	50 cm	CD (Marsden Point)	DML Survey provided by Northport
2024 Ruakaka SBES Survey	Ruakaka transects	Bathymetry	Singlebeam Echosounder	20 m point spacing	NZVD	MetOcean Archive

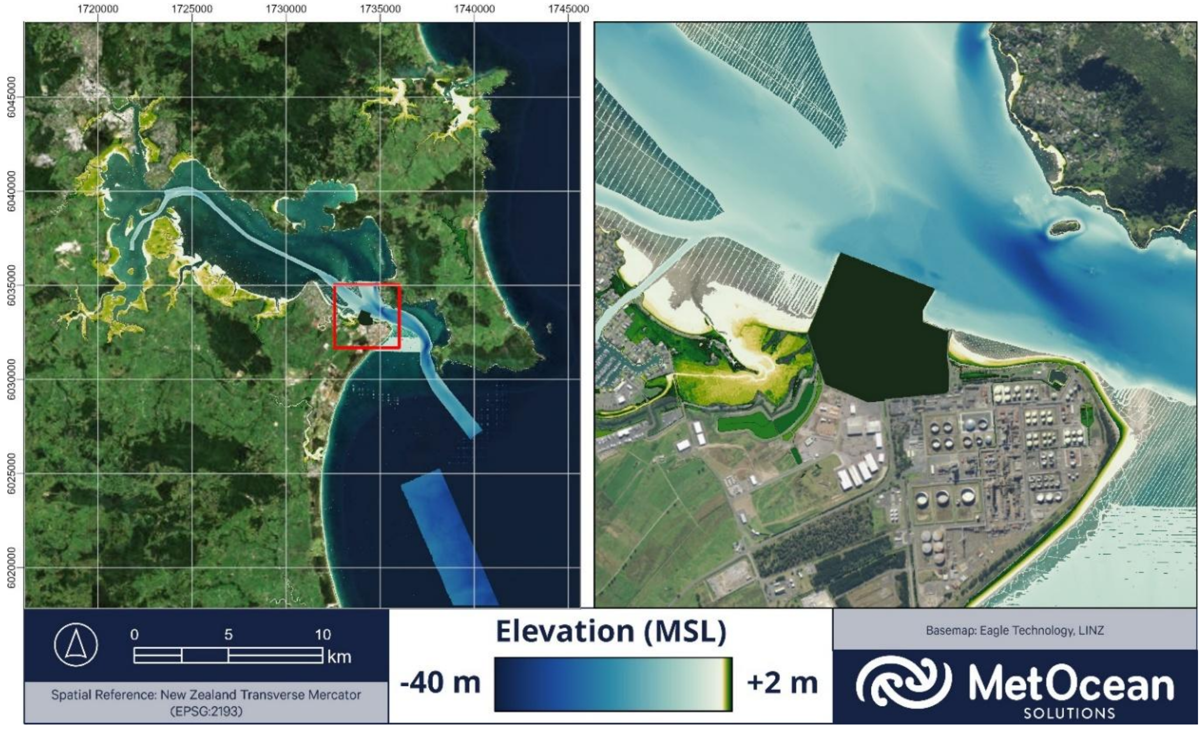

Figure 2-3 High resolution topography and bathymetry data used to update the previously constructed grid.

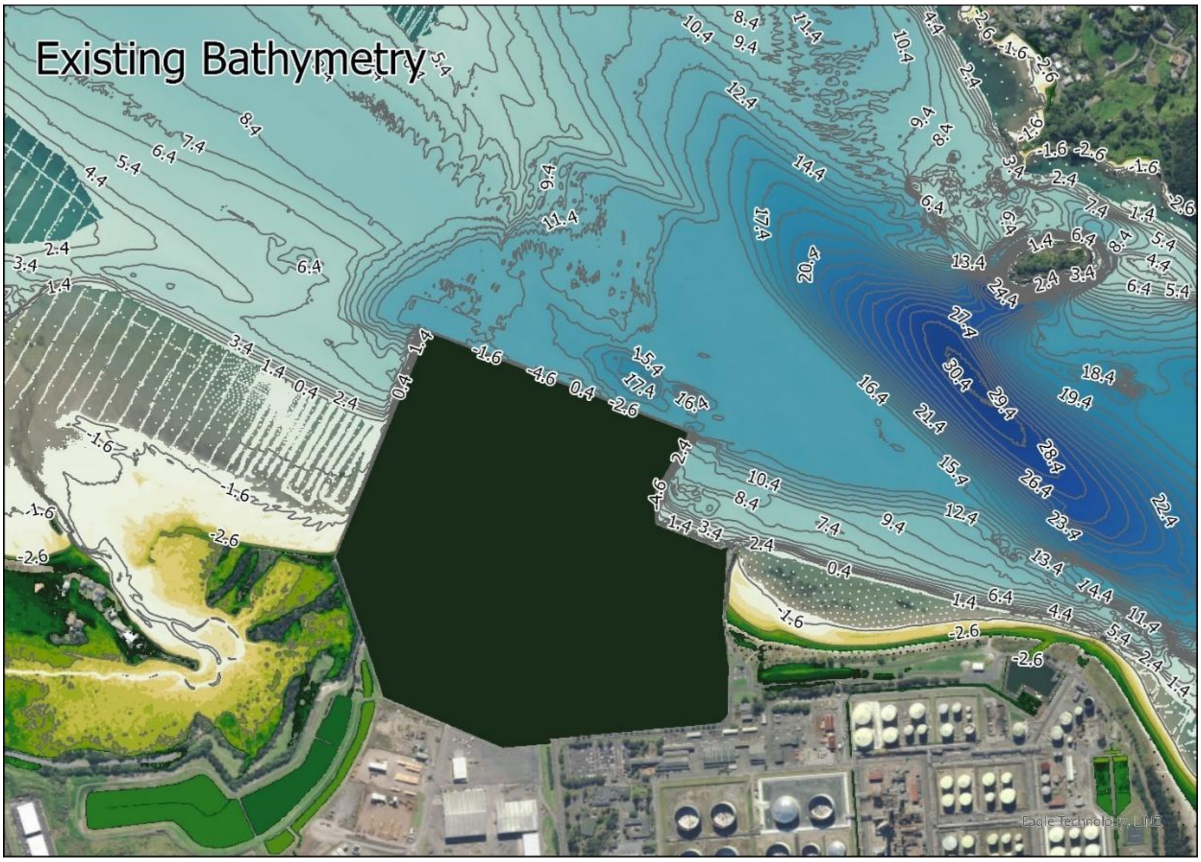

Figure 2-4 Existing bathymetry around Northport. Depths are in metres relative to CD.

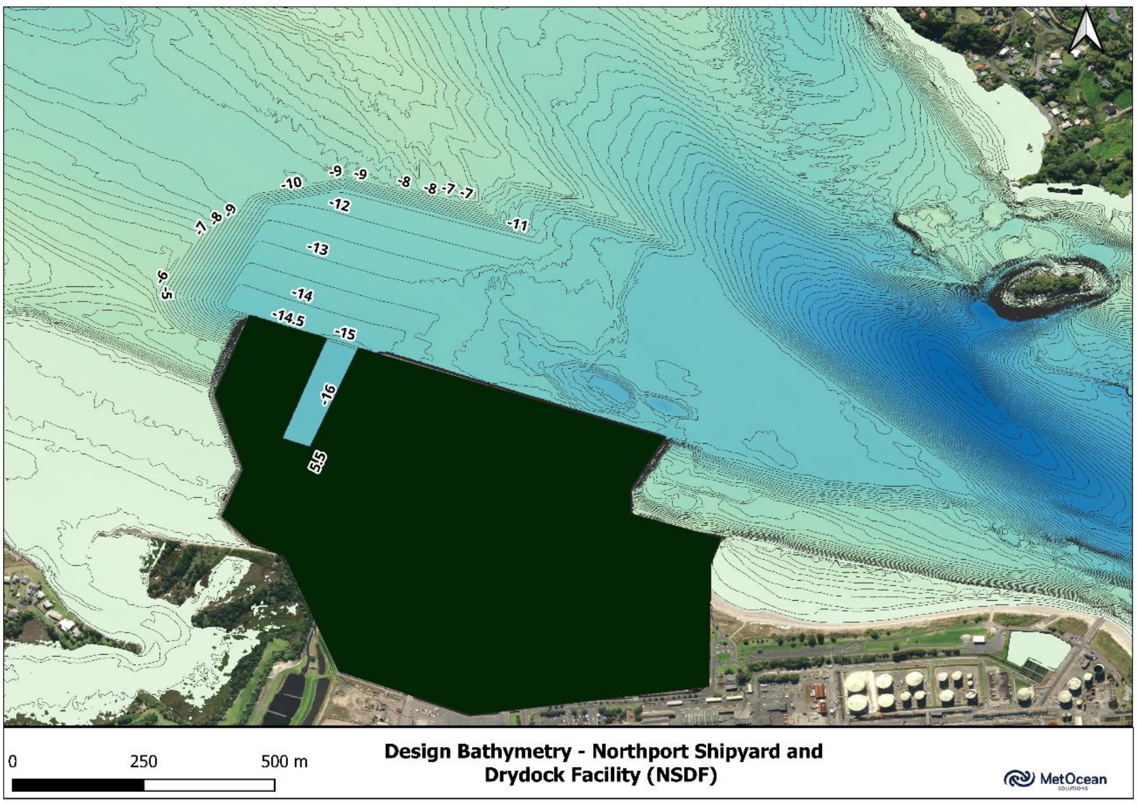

Figure 2-5 Bathymetry around Northport incorporating the Northland Shipyard and Drydock Facility design only. Depths are in metres relative to CD.

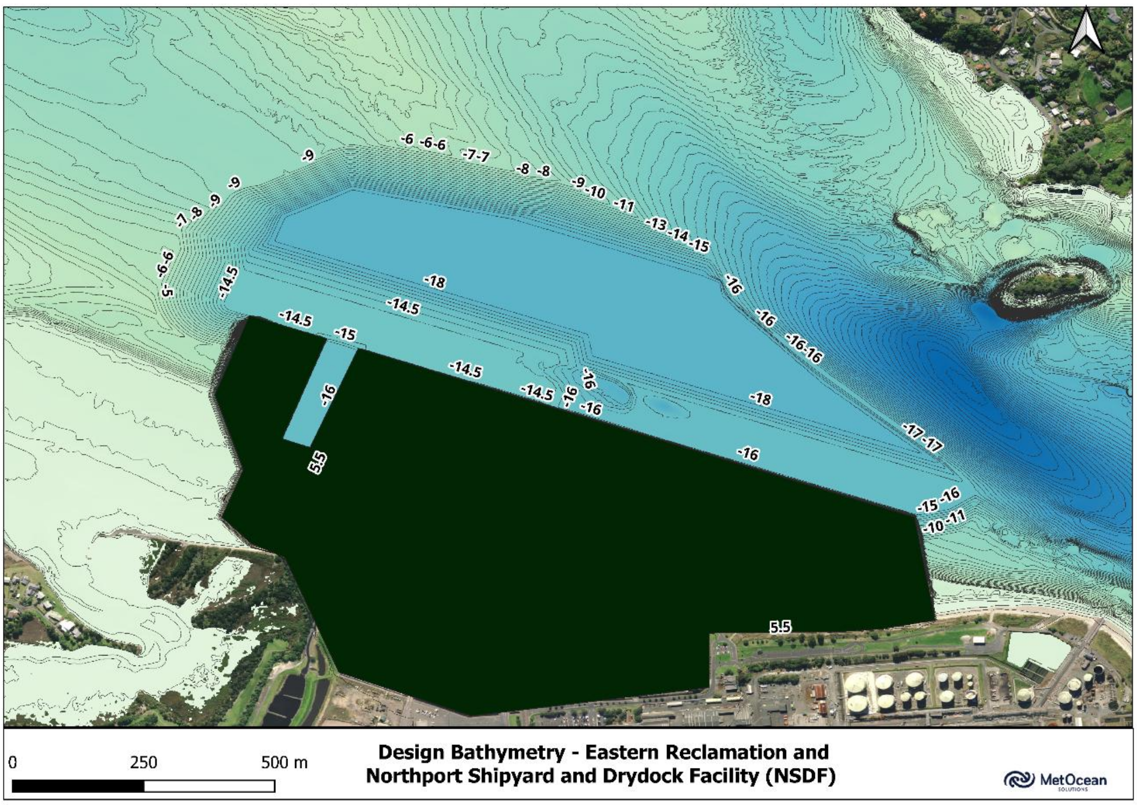

Figure 2-6 Bathymetry around Northport incorporating the Northland Shipyard and Drydock Facility and eastern reclamation designs. Depths are in metres relative to CD.

2.4 Vertical datum

Tide gauge data was used to determine the offset between Chart Datum (CD), Lowest Astronomical Tide (LAT), NZVD2016, and present day mean sea level (MSL), as shown in Figure 2-7. Tidal levels at Marsden Point were sourced from LINZ, which reports that LAT and MSL are 0.17 and 1.63 m above CD respectively. MSL (derived from data collected between 2001-2019) was calculated as 0.136 m below NZVD by Stephens & Paulik (2023). These offsets were used to convert the bathymetry and topographic datasets to a common MSL vertical datum for input to the model.

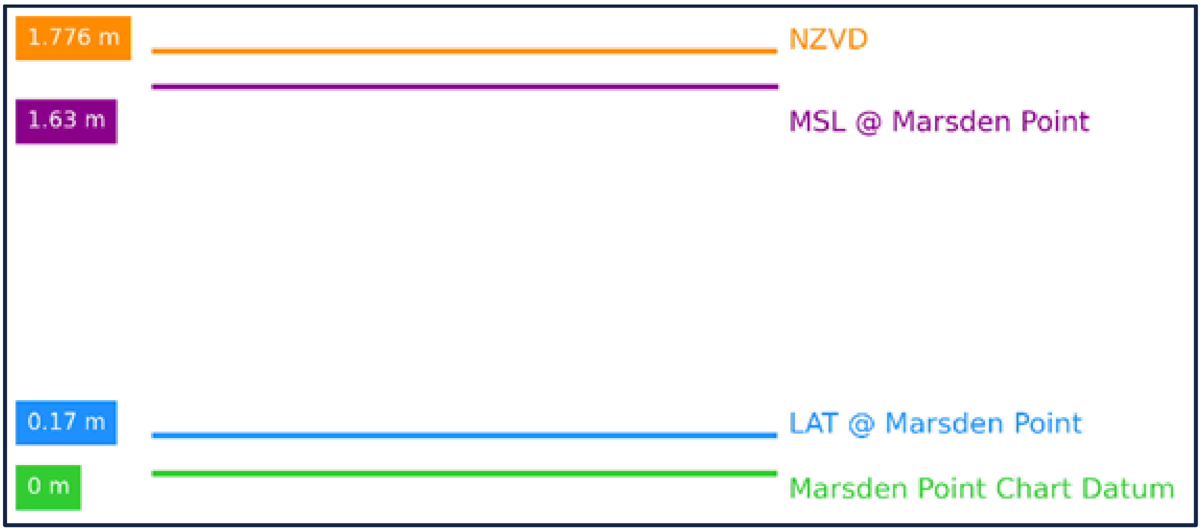

Figure 2-7 Vertical datum relationships at Marsden Point.

3.Methodology

The present study applied the same model setup/configurations used in the previous studies, including computational domain extent and model forcing terms (MetOcean Solutions, 2022a, 2021a, 2018f). By doing so, it is expected that all the previous model features and calibration are retained. Compared to previous studies, the only differences in the model configurations of the present investigation are the use of the updated bathymetry provided by the Port and the mesh refinement around the proposed layout (described in Section 3.2). The purpose of refining the mesh around the proposed dredging and reclamation areas is to capture the shape of the new designed batter slope and the proposed layout. The following sections briefly describe the numerical model framework, computational domain, model forcing inputs, and model verification applied for the present study.

3.1 Model description

This study uses the open-sourced hydrodynamic modelling system: Semi-implicit Cross-scale Hydroscience Integrated System Model (SCHISM) based on Zhang and Baptista (2008); Zhang et al. (2016). It is based on unstructured grid algorithms with the robustness and computational efficiency designed to address various applications across creek-lake-river-estuary-shelf-ocean scales. Specifically, SCHISM does not require any splitting mode and thus excludes the splitting errors which often procedure between internal and external modes. It employs the semi-implicit time stepping with Eulerian-Lagrangian treatment of advection (Zhang and Baptista, 2008) with an implicit transport solver using two limiter functions which have been shown to work with different Courant numbers (Zhang et al., 2016).

The major challenge to coastal modelling is to resolve the complex shoreline and bathymetry in horizontal space. The unstructured models are ideal for this. However, many unstructured grid models use explicit splitting methods which are restricted to the Courant conditions. The stability of these models often requires a small timestep. Further, in 3D ocean modelling, the restriction is often related to the numerical scheme used to solve the vertical dimension. Due to small grid size in the vertical layer, the explicit scheme which is also subjected to the Courant criterion requires a large number of sub-iterations. Generally, explicit ocean models are often computationally more expensive.

Additionally, in 3D mode, SCHISM utilises the Localised Sigma Coordinates (Zhang et al., 2014) (described in a latter section) which maximises the benefits of traditional Z and terrain-following coordinate system while excluding their limitations. Therefore, SCHISM is an ideal modelling system to simulate hydrodynamics for dredging applications such as required in the present study. For reference, the reader may refer to several international studies[3] that used SCHISM model to address dredging impacts including those done by Lopes et al. (2009), Mendes, Fortunato, and Pires-Silva (2016) and Ye et al. (2018b).

3.2 Model domain

The model domain is defined by the horizontal grid shown in Figure 3-1. The grid extends into Bream Bay with water depths on the offshore open boundary of 60 m sufficient to capture ocean tidal dynamics. The mesh resolution varies from a coarse mesh size of approximately 300 m at the open boundary to the finest size of approximately 5 m located nearshore and in the vicinity of the proposed dredged and reclamation areas. Updates to the mesh was undertaken to align to the design contours from both the Design West and Design East and West proposed dredging, reclamation and wharfs (Figure 3-2).

To reflect changes in the bathymetry between the Existing and the two proposed designs, the same computational grid was used for all three simulations.

[3] http://ccrm.vims.edu/schismweb/schism_pubs.html

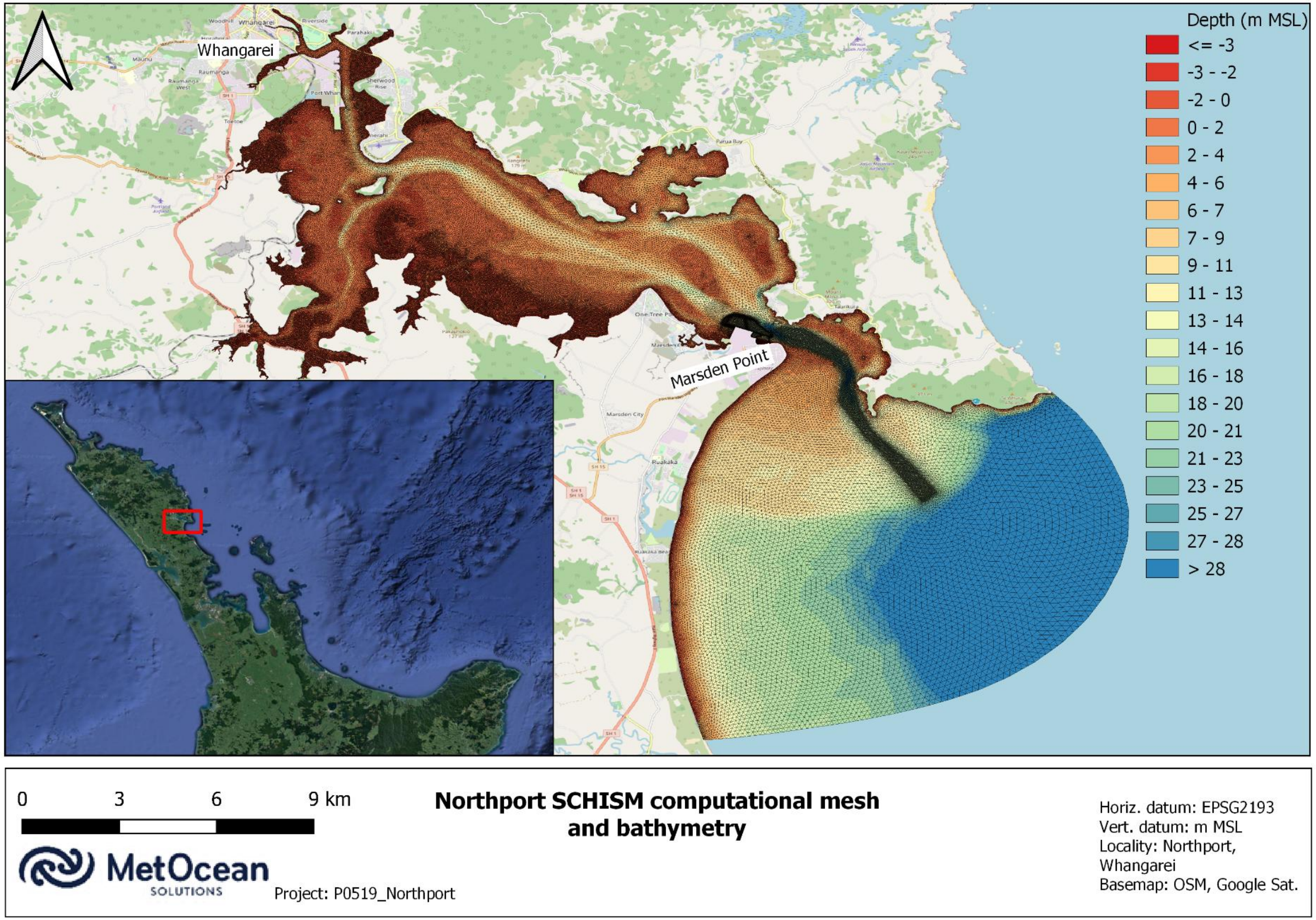

Figure 3-1 SCHISM computational mesh and bathymetry.

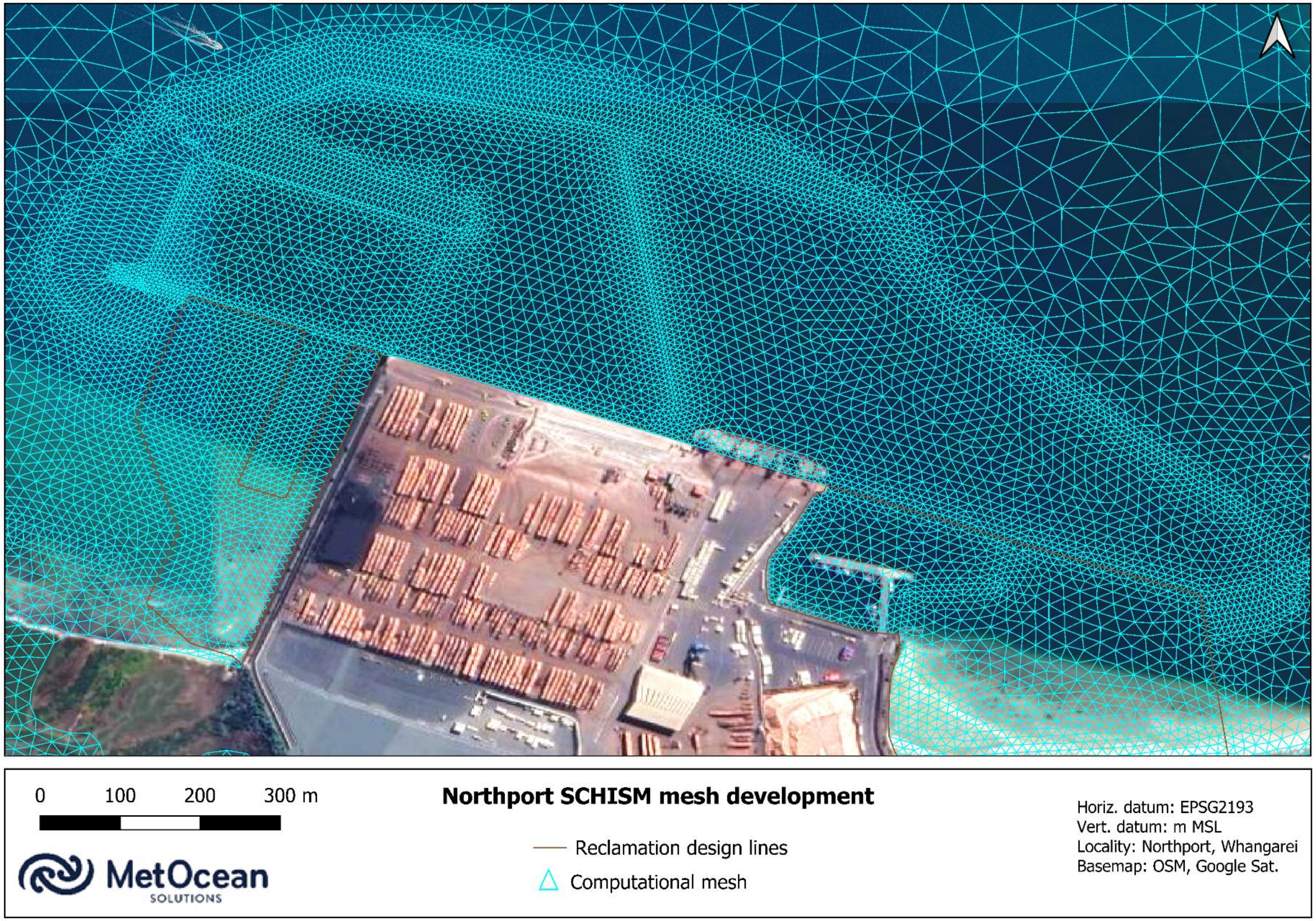

Figure 3-2 SCHISM computational mesh refined and aligned to port designs.

3.3 Model Bathymetry

The updated existing bathymetry was used as the base for the Existing model layout shown in Figure 3-3. The Existing bathymetry layout was then modified to account for the proposed NSDF and Northport's consented eastern expansion as set out in Section 2.2. The interpolated bathymetry is presented in Figure 3-3, Figure 3-4 and Figure 3-5 for the Existing and two proposed layouts respectively.

It is noted that the bathymetry attached to the numerical mesh is relative to mean sea level (MSL) using the linear interpolation method to interpolate to each grid node.

The reporting locations for the model outputs are displayed in Figure 3-3 and Figure 3-5.

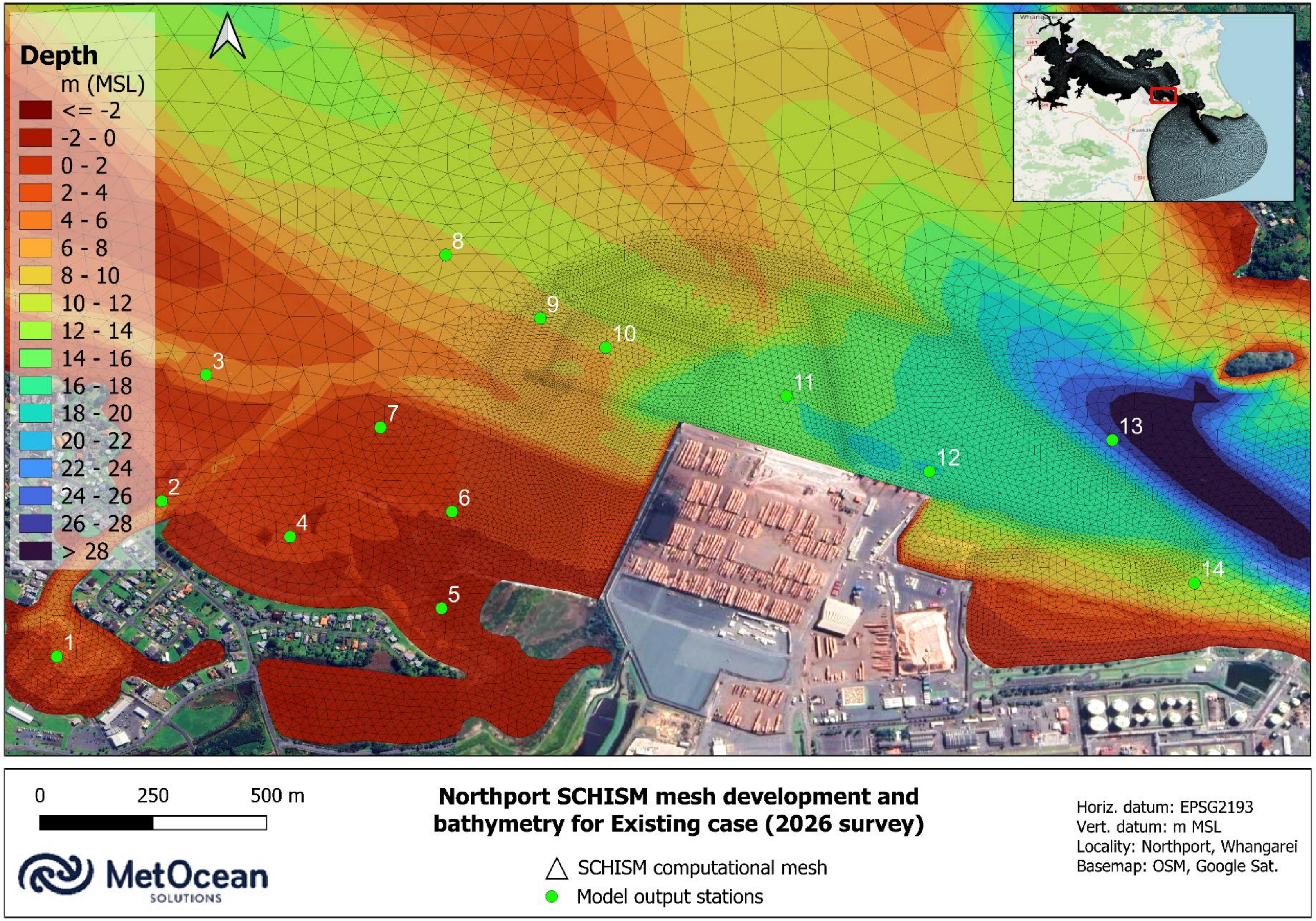

Figure 3-3 SCHISM computational mesh and bathymetry for the Existing case.

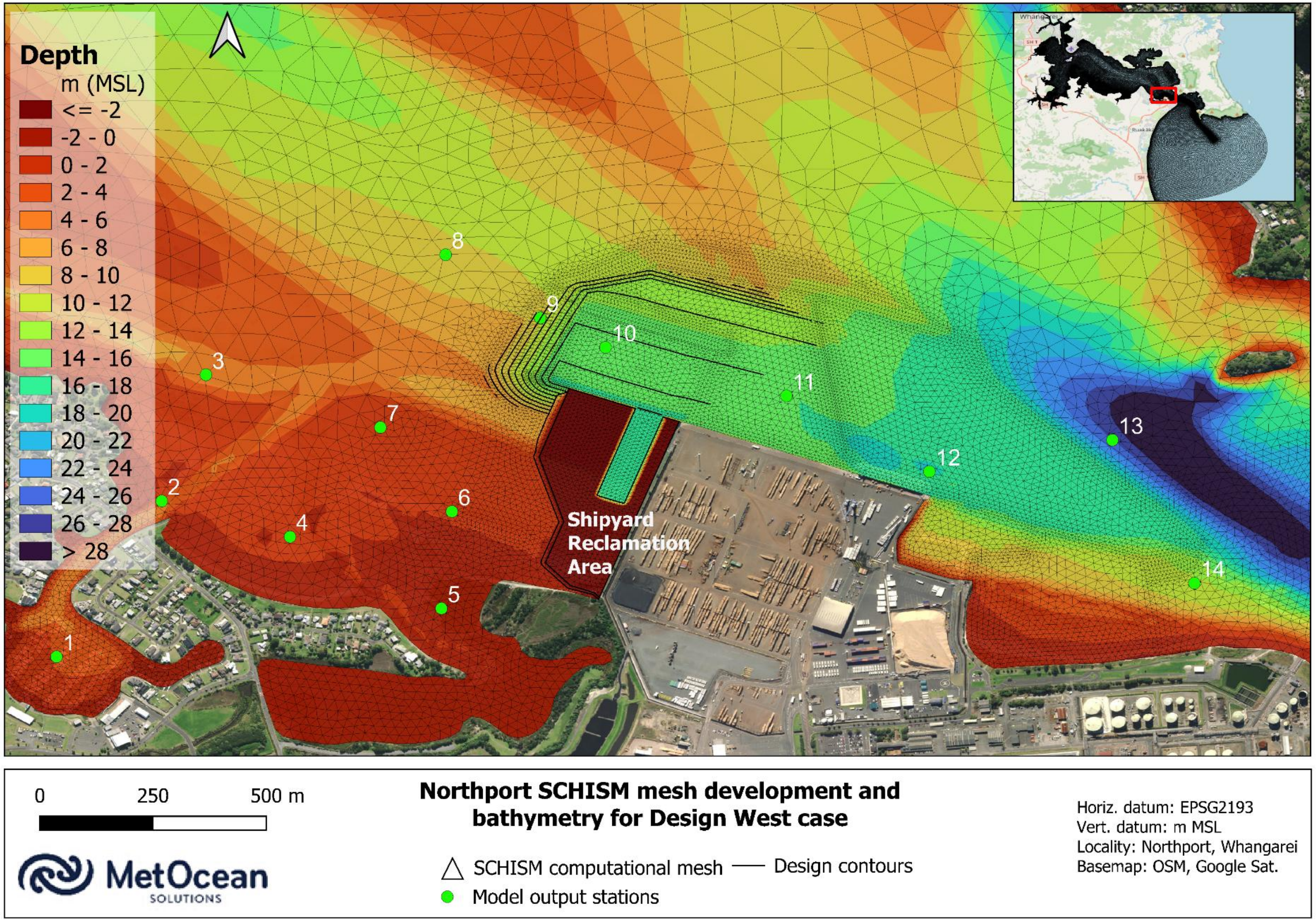

Figure 3-4 SCHISM computational mesh and bathymetry for the Design West case (Northland Drydock and Shipyard Facility).

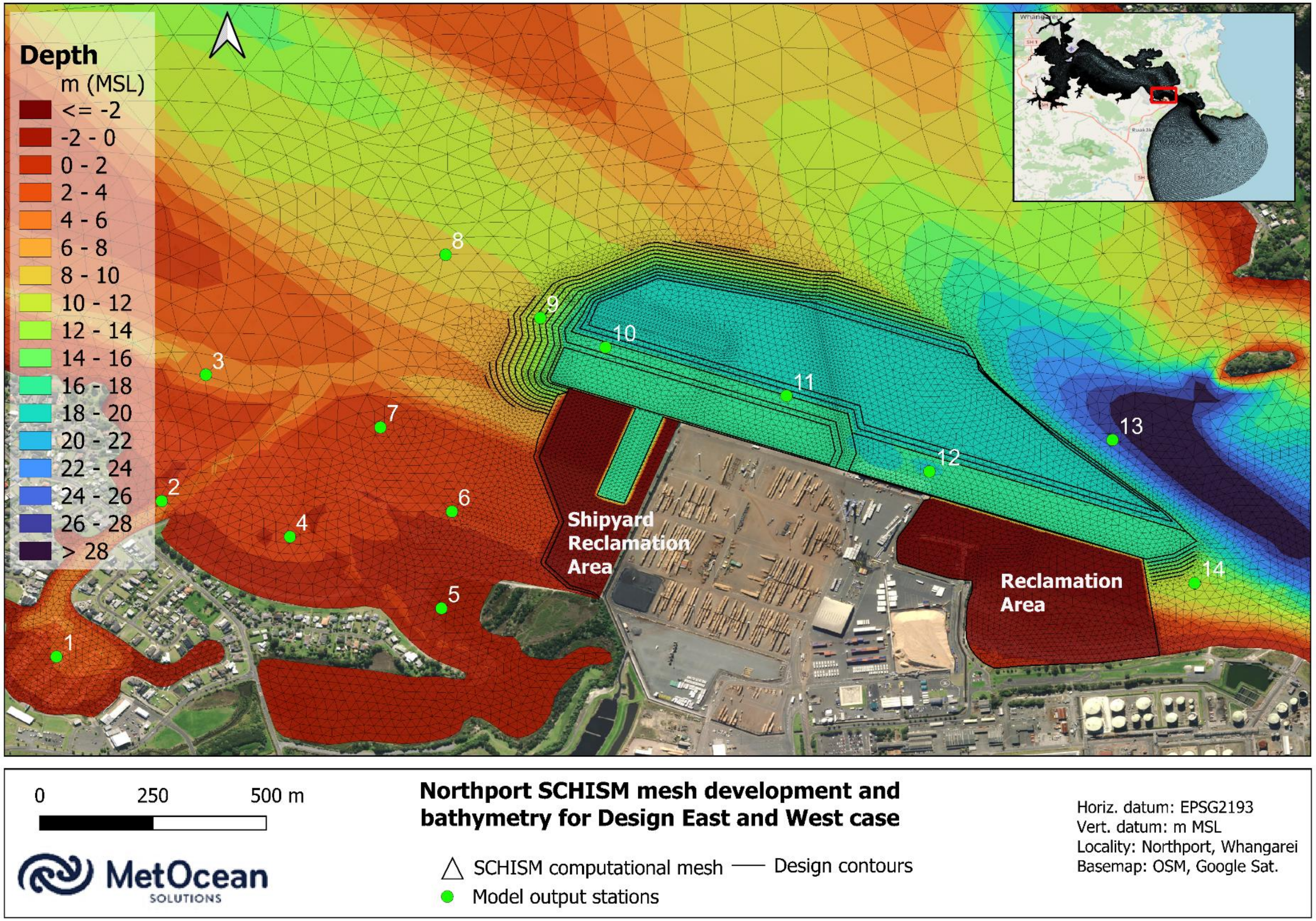

Figure 3-5 SCHISM computational mesh and bathymetry for the Design East and West case (Northland Drydock and Shipyard Facility and the Eastern Development).

3.4 Vertical grid

In this study, SCHISM was configured in 3D mode and thus requires a vertical grid or vertical coordinate system to be described. In ocean modelling, the importance of the vertical coordinate system has long been identified. Currently, there are three commonly used vertical coordinates namely Z, terrain-following, and pressure coordinates. However, these coordinate systems each have their own limitations (e.g. see Song and Hou (2006) for a review). For instance, Z-coordinates often creates artificial staircases resulting in artificial drag. Similarly, the terrain-following coordinate systems often have a problem with the pressure gradient discretization leading to spurious flow. Among the less commonly used vertical coordinate systems, the isopycnal and pressure-coordinate approaches encounter challenges in preserving mass within well-mixed zones.

For this study, a Localised Sigma Coordinates with Shaved Cell (LSC^2) developed by Zhang et al. (2014) is used to eliminate the above issues. After this development, the LSC^2 vertical grid has been widely used in the SCHISM modelling community[4] including studies by Ye et al. (2016), Ye et al. (2018a), Zhang et al. (2020) and Liu et al. (2020). This is the most advanced vertical grid system which has benefits from both the terrain-following and Z-coordinate systems making 3D SCHISM models very efficient in terms of computational resources. Furthermore, smoothness features in the LSC^2 grid are designed to eliminate the staircase problem caused by the mismatch between vertical layers. This problem is commonly found in other traditional vertical grid systems applied for coastal domains where the bathymetry is often complex. An example for the LSC^2 grid used in this project is shown in Figure 3-6.

---

[4] http://ccrm.vims.edu/schismweb/

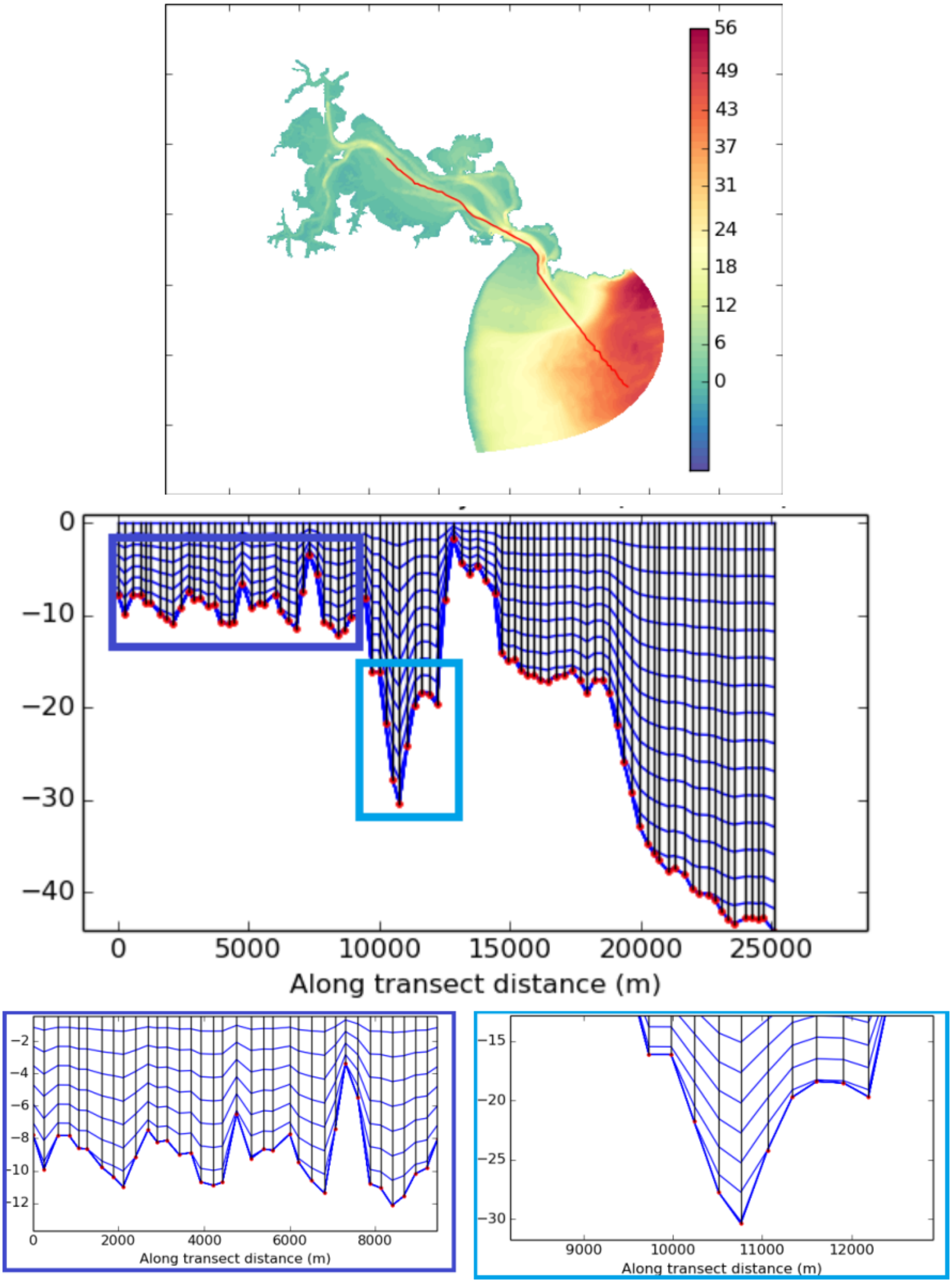

Figure 3-6 The design of a LSC[2] vertical grid for 3D SCHISM model. The top panel presents a cross section (red line) along the main channel over the horizontal domain. The vertical grid along this section shows in the middle panel. Two zoomed sections (in rectangular boxes) are plotted in the bottom panel.

3.5 Model inputs

The computational domain has an open boundary on the ocean side which requires tidal conditions to be prescribed. In the present study, SCHISM was forced with tidal constituents at open boundary grid points. These constituents were derived from a one-year ROMS model simulation of the environs with a spatial resolution of 0.3 km. The velocity, residual components, salinity, and temperature were also interpolated into the 3D SCHISM grid from the same ROMS model.

Sensitivity analysis undertaken as part of the previous hydrodynamic modelling (MetOcean Solutions, 2021a) assessed the effects of wind forcing on currents and described the subsequent inclusion of wind forcing in the simulations. As in the previous modelling, the near-surface wind field was prescribed by a 36-year (1979-2014) regional atmospheric hindcast carried out by MOS. The WRF (Weather Research and Forecasting) model was established over all of New Zealand at hourly intervals and approximately 12 km resolution. The hindcast was specifically tuned to provide highly accurate marine wind fields for metocean studies around New Zealand. The WRF model boundaries were sourced from the CFSR (Climate Forecast System Reanalysis) dataset distributed by NOAA (Saha et al., 2010), which was available at hourly intervals and 0.31° spatial resolution.

While the WRF hindcast produced atmospheric parameters at hourly intervals over the 36 years, only the near surface wind field (i.e. 10-minute mean at 10 m elevation) are used in the study. Validation of the WRF reanalysis has been undertaken at various locations around New Zealand. More details about model inputs can be found in the final report written for Refining New Zealand project (MetOcean Solutions, 2019).

Each simulation used a hotstart file which was generated using a 3-day simulation to remove the need for a model warmup period. Both the model map and station timeseries outputs were produced at 10-minute intervals.

4. Results

As tidal forcing dominates the climatology at the site, hydrodynamic simulations were undertaken over a 29-day full lunar cycle (2 spring/neap cycles). The modelled period was retained from the previous modelling reports of 1st -30th January 2015. Simulations of the two proposed designs were compared to Existing simulations to determine any potential impacts of the proposed design on hydrodynamics at the site. The effects of the Design West are presented in Section 4.1 and the Design East and West are presented in Section 4.2.

4.1 Effects of Design West on hydrodynamics

Comparison of the modelled water levels and currents between the Existing and Design West simulations over the full simulation period are assessed at selected station output locations. Station output locations and depths are displayed in Figure 3-3 and Figure 3-4. The tidal planes at two stations are displayed in Table 4-1, showing no changes at station 3 in Blacksmith Creek while a 0.01 m decrease in the HAT is predicted at station 10 within the dredge footprint.

A statistical analysis of the current speeds at selected stations are provided in Table 4-2. The largest change in current speeds is at station 10 with the 98th percentile current speeds of 1.07 $m.s^{-1}$ and 0.96 $m.s^{-1}$ for the Existing and Design West simulations respectively. The percentage difference in mean current speeds is a 18.8% reduction due to the increased depth between the two simulations from 8.4 m to 15.0 m respectively (MSL). The other stations all had changes in mean current speeds of 2.7% or less.

Timeseries of the modelled Existing and Design West water levels, current speeds and directions for the full simulation period at selected stations are displayed in Figure 4-1, Figure 4-2 and Figure 4-3.

Table 4-1 Tidal planes (m) relative to MSL for Existing and Design West simulations derived over 29-day lunar cycle for selected stations.

Parameter	**Station 3**		**Station 10**	
	Existing (m)	Design West (m)	Existing (m)	Design West (m)
HAT (Highest Astronomical Tide)	1.30	1.30	1.30	1.29
MHWS (Mean High Water Springs (M2+S2))	1.03	1.03	1.02	1.02
MHWN (Mean High Water Neaps (M2-S2))	0.77	0.77	0.76	0.76
MSL (Mean Sea Level)	0.00	0.00	0.00	0.00
MLWN (Mean Low Water Neaps (-M2+S2))	-0.77	-0.77	-0.76	-0.76
MLWS (Mean Low Water Springs (-M2-S2))	-1.03	-1.03	-1.02	-1.02
LAT (Lowest Astronomical Tide)	-1.31	-1.31	-1.30	-1.30

Table 4-2 Current speed statistics ($m.s^{-1}$) for Existing and Design West simulations derived over 29-day lunar cycle for selected stations.

Station	Simulation	Mean	80th %tile	90th %tile	95th %tile	98th %tile	Max	% diff. in mean
Station 3	Existing	0.16	0.22	0.27	0.31	0.34	0.41	-2.1%
	Design West	0.16	0.22	0.26	0.30	0.33	0.41	
Station 8	Existing	0.53	0.75	0.84	0.91	0.99	1.08	0.8%
	Design West	0.54	0.76	0.85	0.93	1.01	1.10	
Station 10	Existing	0.57	0.80	0.89	0.99	1.07	1.22	-18.8%
	Design West	0.46	0.67	0.78	0.87	0.96	1.07	
Station 11	Existing	0.55	0.78	0.92	1.00	1.09	1.25	0.6%
	Design West	0.55	0.78	0.90	1.00	1.09	1.23	
Station 12	Existing	0.49	0.68	0.82	0.93	1.02	1.21	2.7%
	Design West	0.50	0.69	0.82	0.92	1.02	1.18	
Station 13	Existing	0.55	0.78	0.91	1.01	1.16	1.35	-1.2%
	Design West	0.55	0.77	0.89	0.98	1.11	1.31	
Station 14	Existing	0.45	0.64	0.75	0.85	0.96	1.27	1.7%
	Design West	0.46	0.66	0.77	0.86	0.95	1.26	

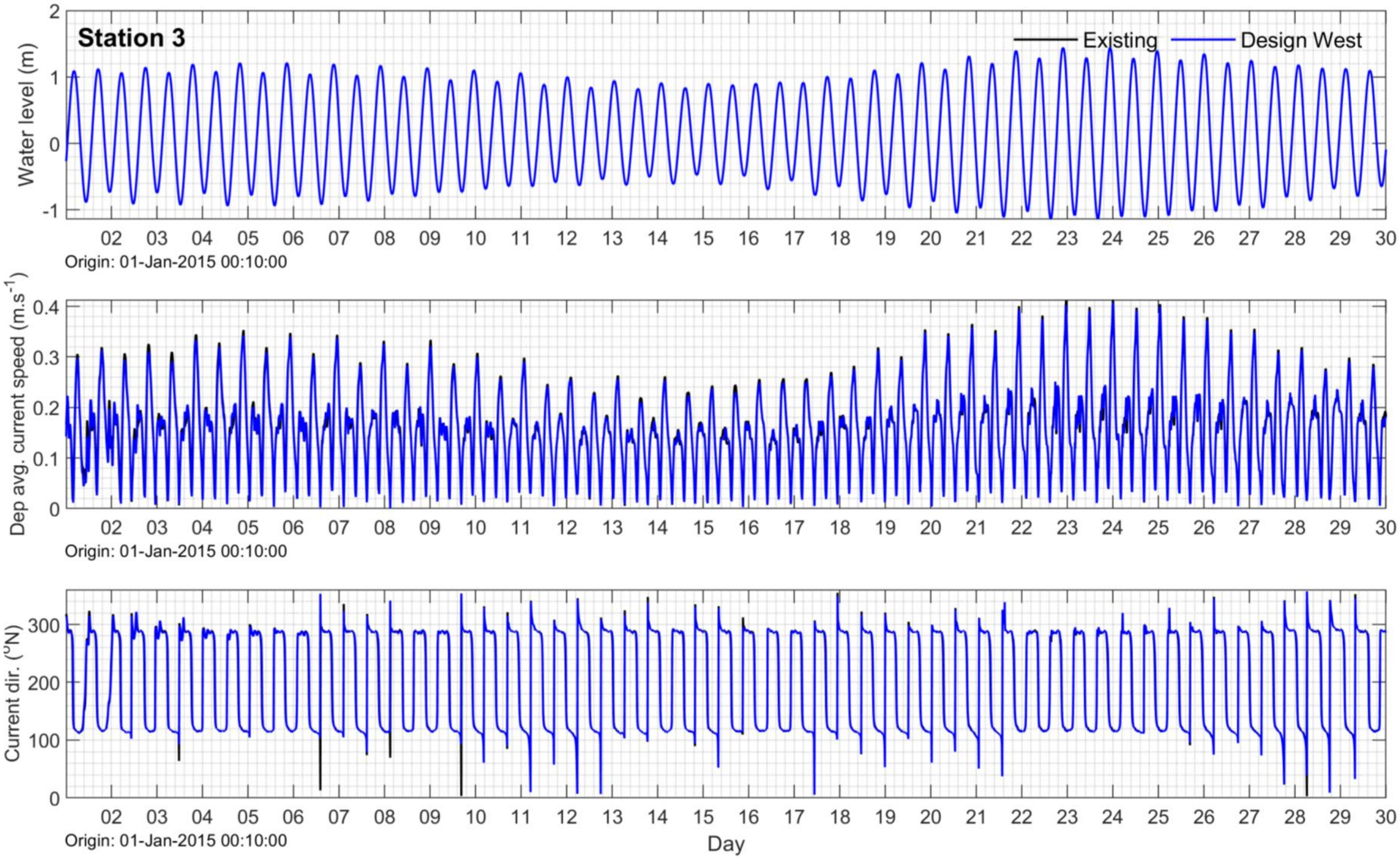

Figure 4-1 Comparison of Existing and Design West simulation water levels, current speeds and directions for the full simulation period at station 3.

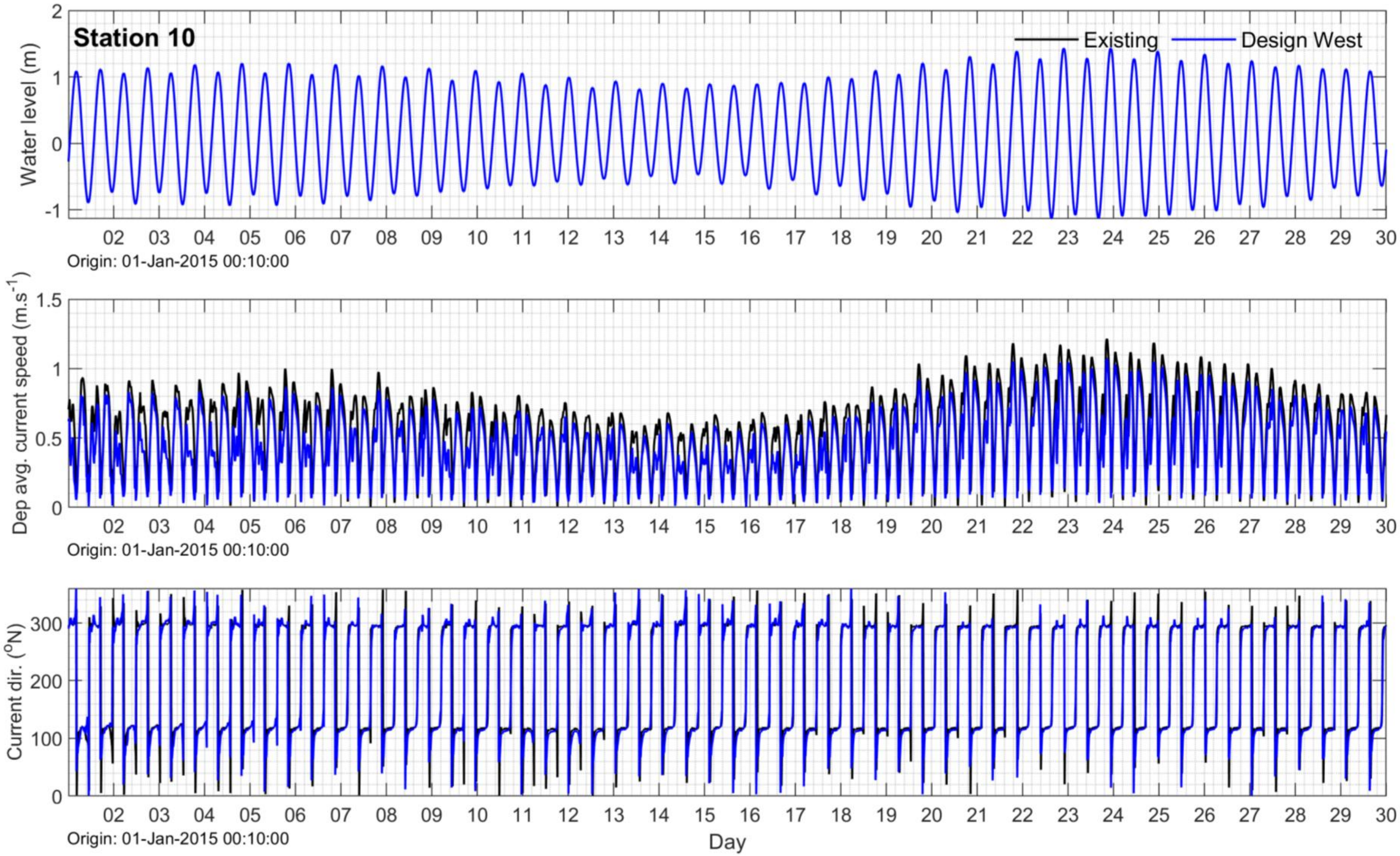

Figure 4-2 Comparison of Existing and Design West simulation water levels, current speeds and directions for the full simulation period at station 10.

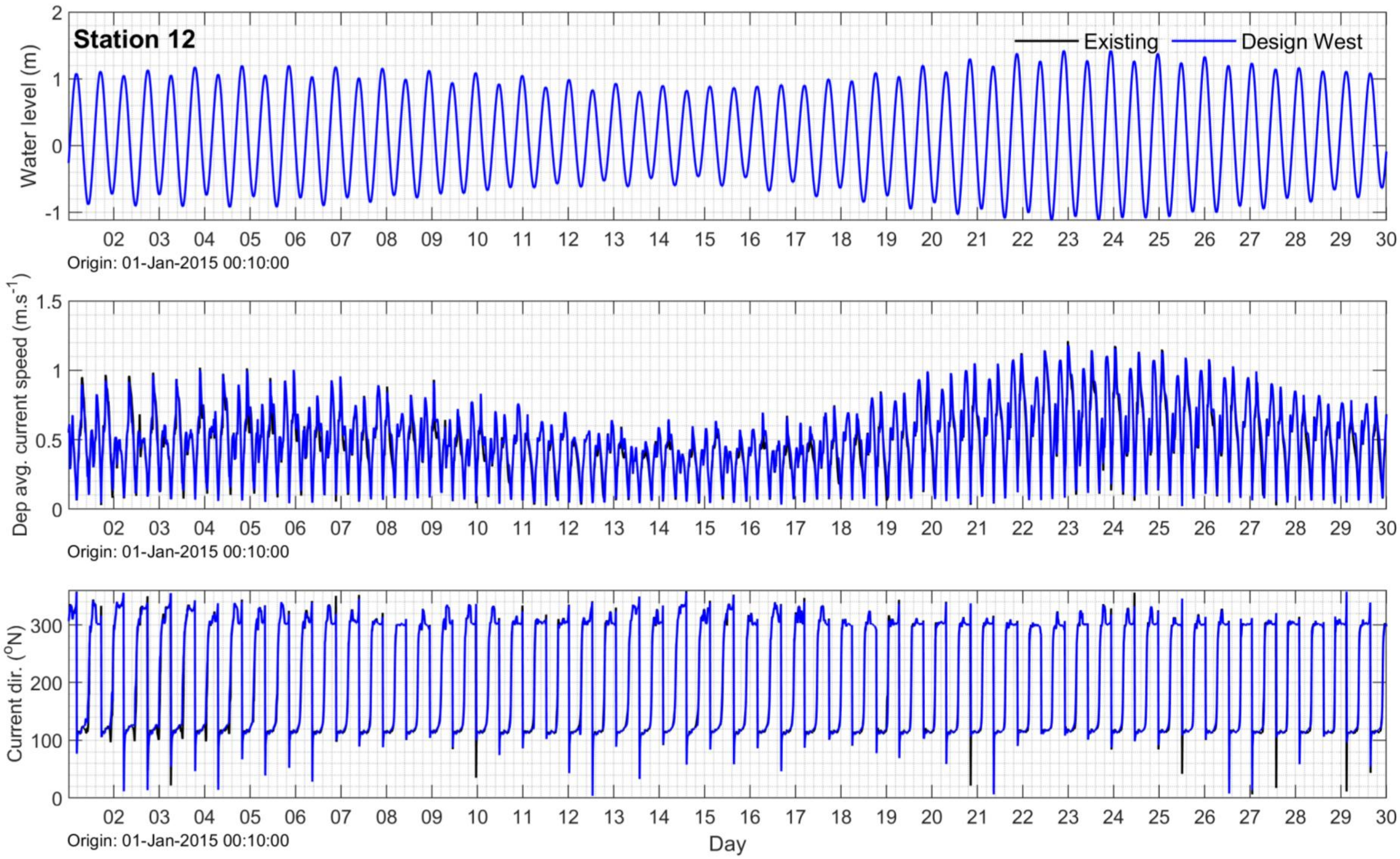

Figure 4-3 Comparison of Existing and Design West simulation water levels, current speeds and directions for the full simulation period at station 12.

4.1.1 Spring tidal cycle

Modelled depth averaged current vectors during spring tide for the Existing and the proposed Design West layout at peak flood are provided in Figure 4-4 and at peak ebb in Figure 4-5. The predicted change in current magnitude between the two options (Design West-Existing) is presented in Figure 4-6 and Figure 4-7 for the flood and ebb tide respectively. Potential changes less than 0.01 $m.s^{-1}$ are masked as they are within the magnitude of model error and were not considered as a meaningful change.

During a peak flood and ebb tide, the potential reduction in current speed is predicted to be less than 0.3 $m.s^{-1}$ for the majority of the study area, with localised areas of 0.7 $m.s^{-1}$. A decrease in current speeds is observed within the following areas:

- A reduction within the western dredge footprint. Currents speeds decreased in this area due to the increase in depth between the two simulations. The change in depth varies across the footprint but is 8.4 m to 15.0 m MSL at station 10.
- A reduction of 0.1 $m.s^{-1}$ to 0.5 $m.s^{-1}$ at the western edge of the proposed reclamation as the flood tide is diverted around the reclamation and on an ebb tide in the lee of the reclamation,
- On an ebb tide, a reduction in current speed less than 0.2 $m.s^{-1}$ in the area around Blacksmith Creek.

Modelled results also show a slight increase in current speeds in some areas during the peak flood and ebb tides. The potential increase in current speeds on a flood and ebb tide is predicted to be less than 0.2 $m.s^{-1}$ in the majority of the study area, with localised areas with an increase of 0.5 $m.s^{-1}$. An increase in current speeds is observed within the following areas:

- Increased current speeds to the west of the dredge footprint less than 0.2 $m.s^{-1}$;
- The largest increase in current speeds is seen alongside the existing berths during an ebb tide with up to 0.5 $m.s^{-1}$ increase; and
- On a flood tide, there are negligeable increases in current speed less than 0.1 $m.s^{-1}$ in the areas around Blacksmith Creek.

Further, comparisons of current magnitudes for a spring tide over 13 hours at 14 locations in the vicinity of the port are shown in Figure 4-8. In terms of magnitudes, the potential changes within Blacksmith creek environs can be determined at stations 1-7. Stations 1-5 and 7 show less than 0.05 $m.s^{-1}$ of change during both a flood (increased speeds) and ebb tide (reduced speeds). At station 6 which is upstream of the shipyard/reclamation, there is a reduction in current speeds of around 0.2 $m.s^{-1}$ after high water which is in keeping with the differences displayed in Figure 4-7 during an ebb tide.

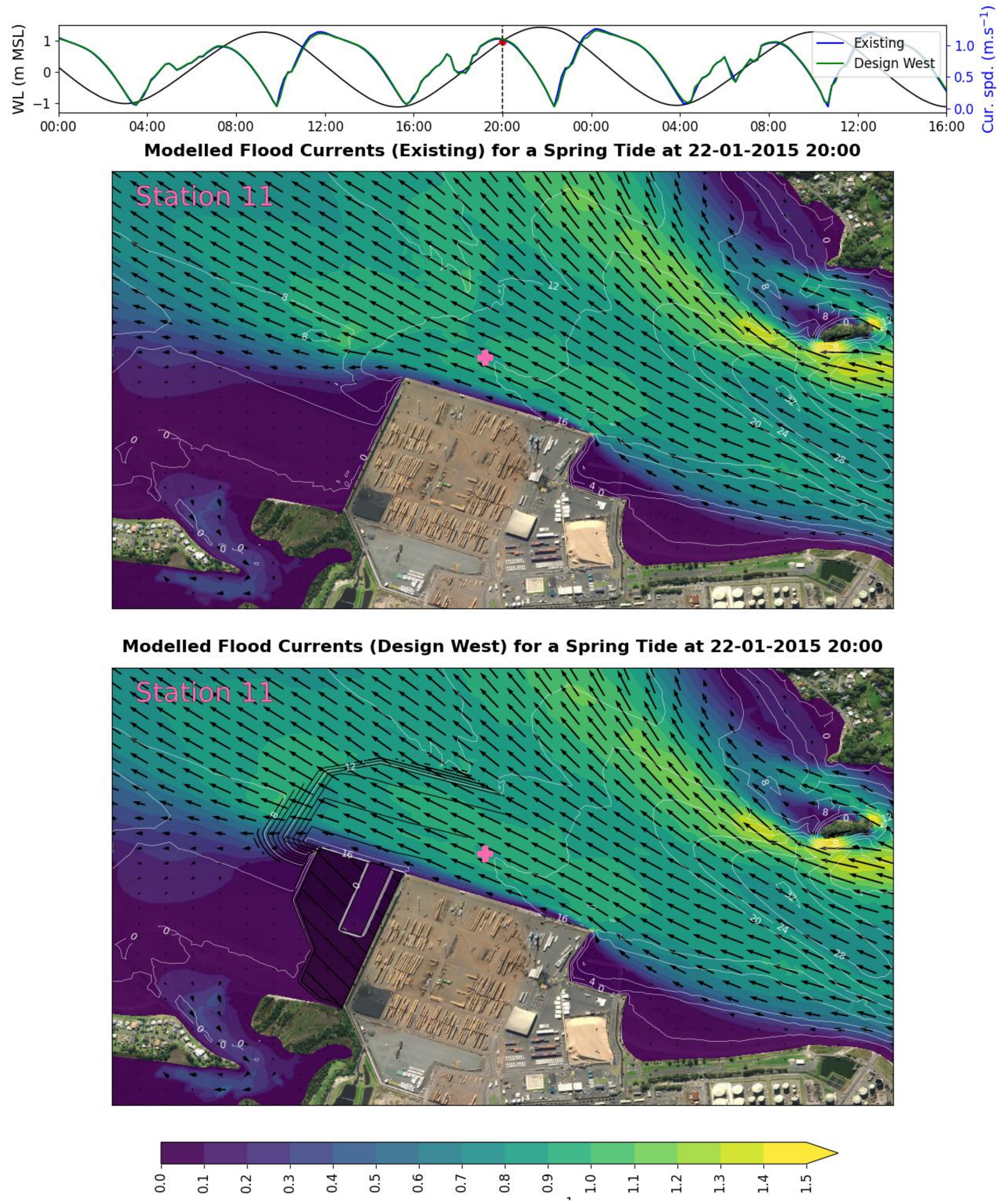

Figure 4-4 Modelled current vectors for the Existing (top) and Design West layout (bottom) during the peak of a flood spring tide and the bathymetry and depth contours used in each simulation. Black design lines display the proposed reclamation and dredging.

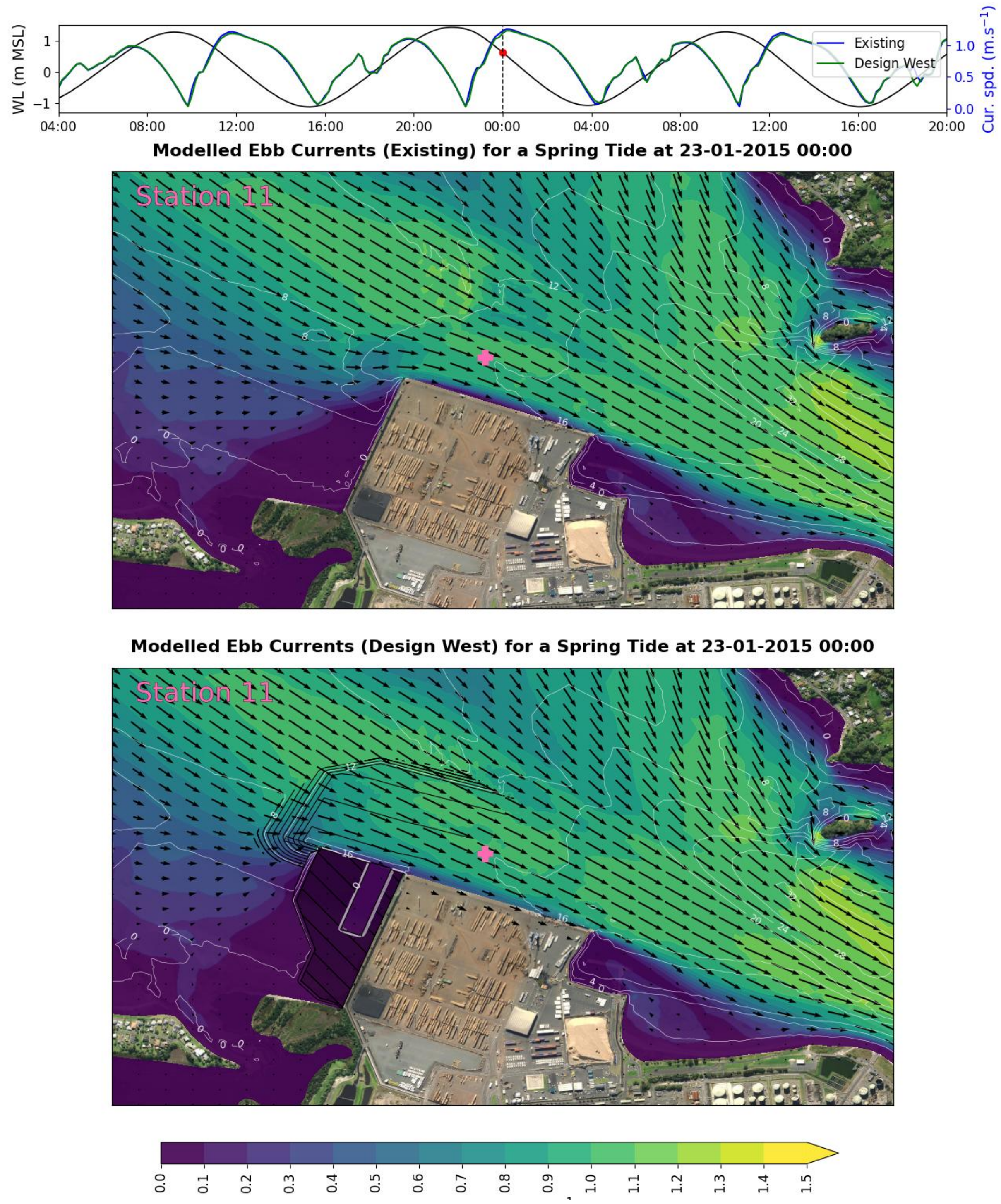

Figure 4-5 Modelled current vectors for the Existing (top) and Design West layout (bottom) during the peak of an ebb spring tide and the bathymetry and depth contours used in each simulation. Black design lines display the proposed reclamation and dredging.

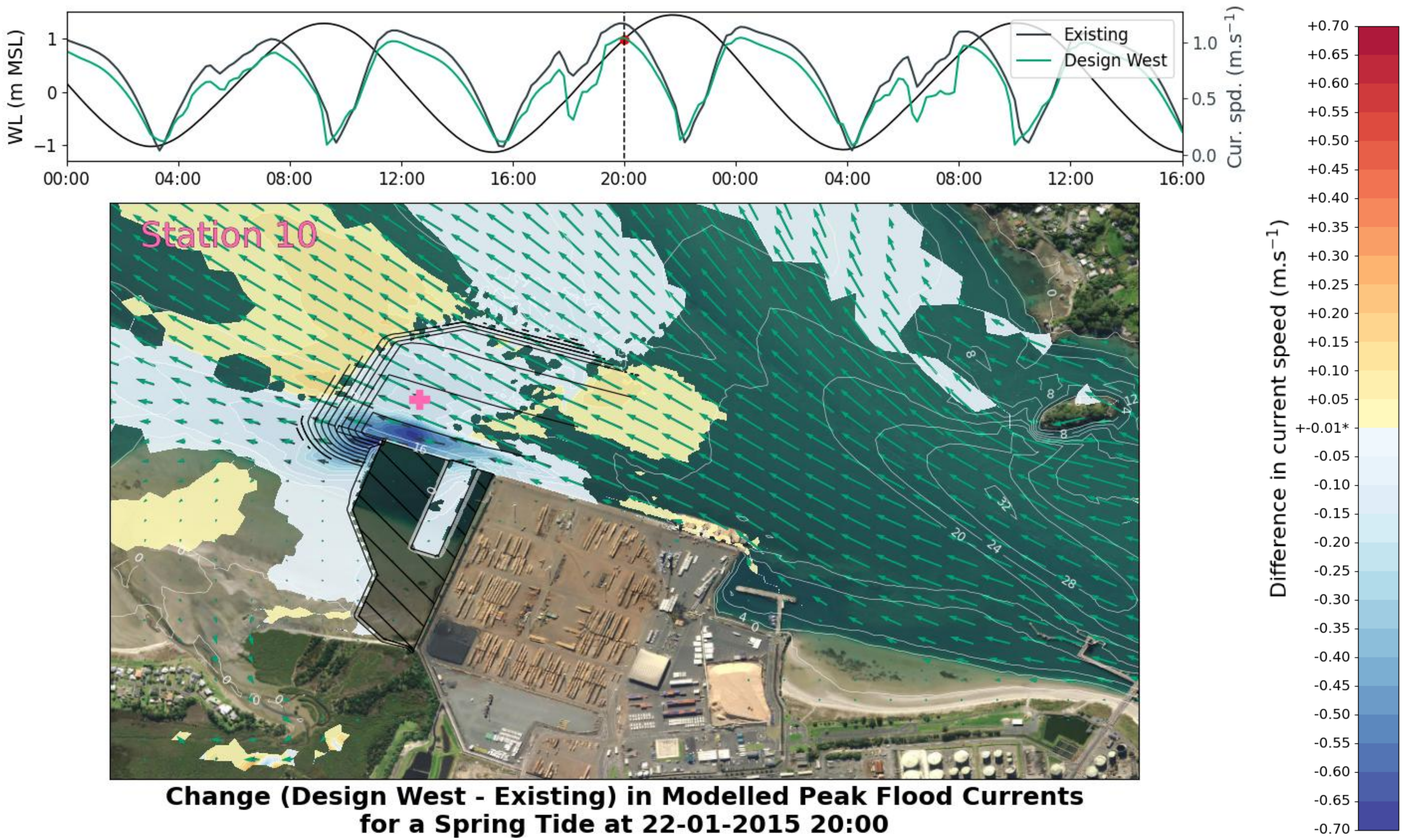

Figure 4-6 Modelled current vectors for the Existing and Design West layout and difference in current magnitude during the peak of a flood spring tide. Note potential changes less than 0.01 $m.s^{-1}$ are masked as they are within the magnitude of model error and were not considered as a meaningful change.

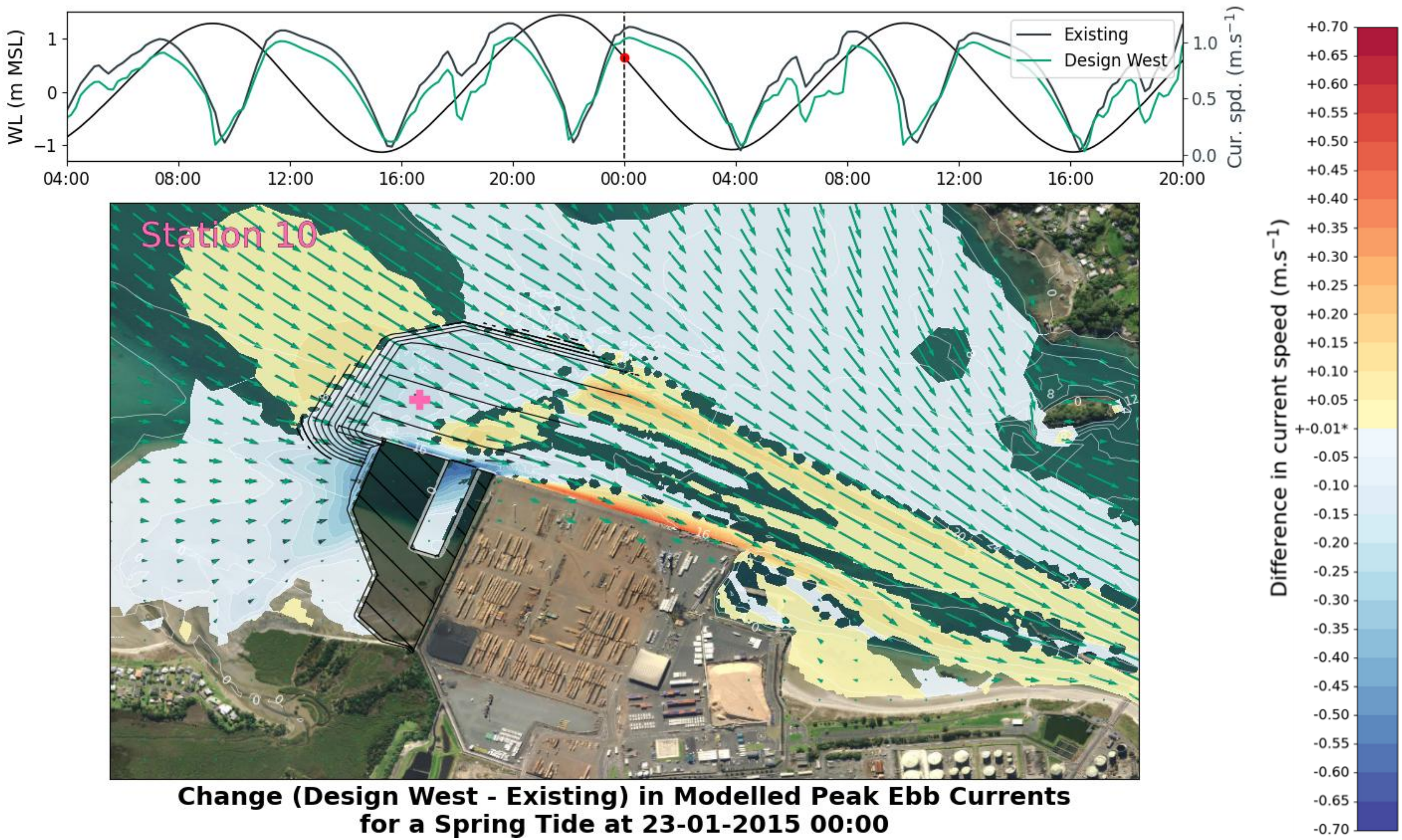

Figure 4-7 Modelled current vectors for the Existing and Design West layout and difference in current magnitude during the peak of an ebb spring tide. Note potential changes less than 0.01 m.s^{-1} are masked as they are within the magnitude of model error and were not considered as a meaningful change.

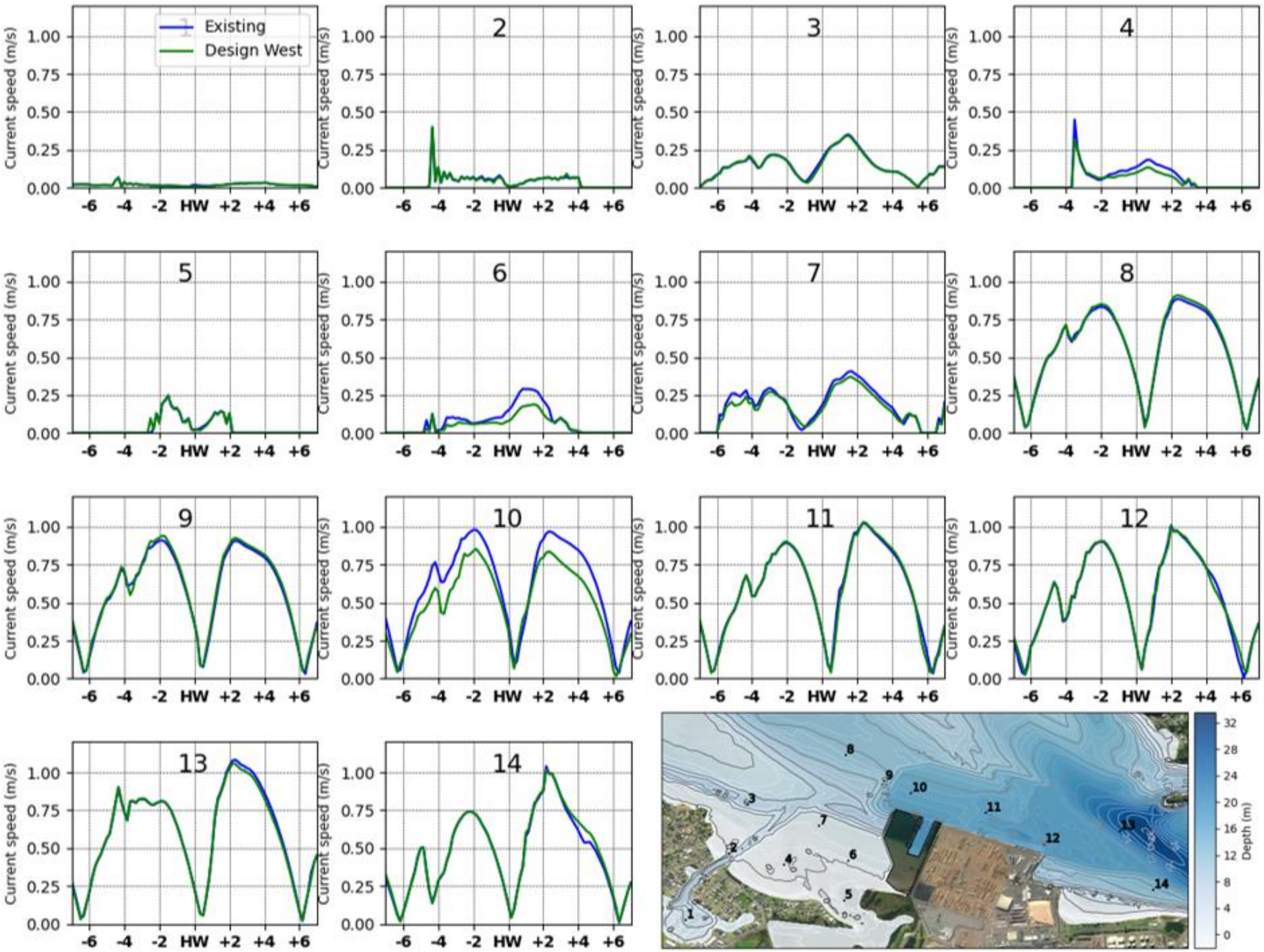

Figure 4-8 Comparisons between modelled current magnitudes for the Existing and Design West layout for 13 hours of a typical spring tidal cycle.

4.1.2 Neap tidal cycle

Modelled current vectors during a neap tide for the Existing and the Design West are displayed at peak flood in Figure 4-9 and at peak ebb in Figure 4-10. The predicted change in current magnitude between the two options (Design West-Existing) is presented in Figure 4-11 and Figure 4-12 for the flood and ebb tide respectively. In terms of magnitude, the current speed near the project site is about 0.5-0.6 $m.s^{-1}$ during a neap tide, which is approximately half the speed observed during spring. As a result, the potential changes to current speeds during a neap tide are less than during a spring tide.

Similar patterns are seen, with the reduction occurring within the dredge footprint for both a flood and ebb tide. A potential increase in current speeds to the west of the dredge footprint on a flood tide and alongside the existing berths on an ebb tide are expected (see Figure 4-11 and Figure 4-12).

Further, comparisons of current magnitudes for a neap tide over 13 hours at 14 locations in the vicinity of the port are shown in Figure 4-13.

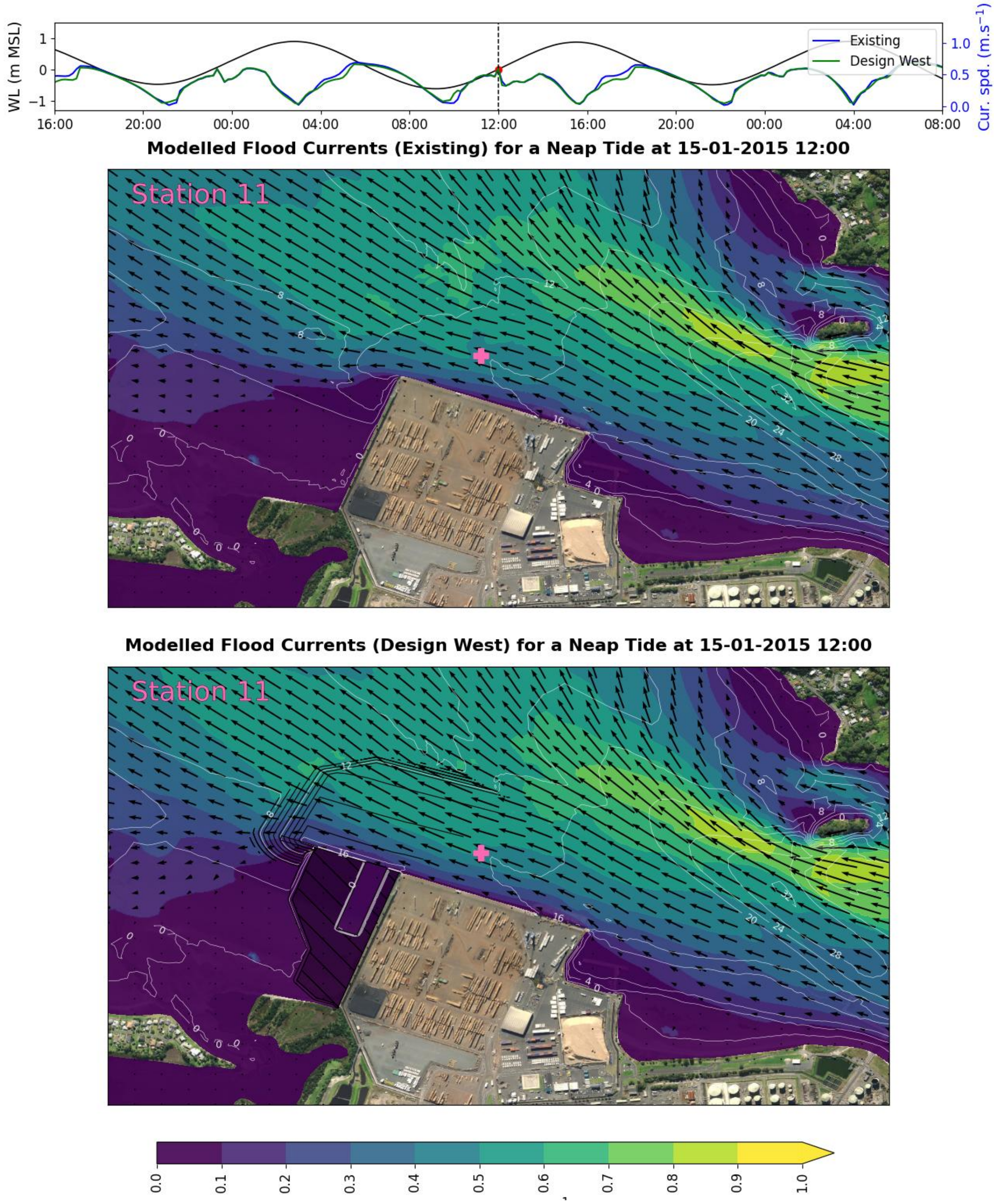

Figure 4-9 Modelled current vectors for the Existing (top) and Design West layout (bottom) during the peak of a flood neap tide and the bathymetry and depth contours used in each simulation. Black design lines display the proposed reclamation and dredging.

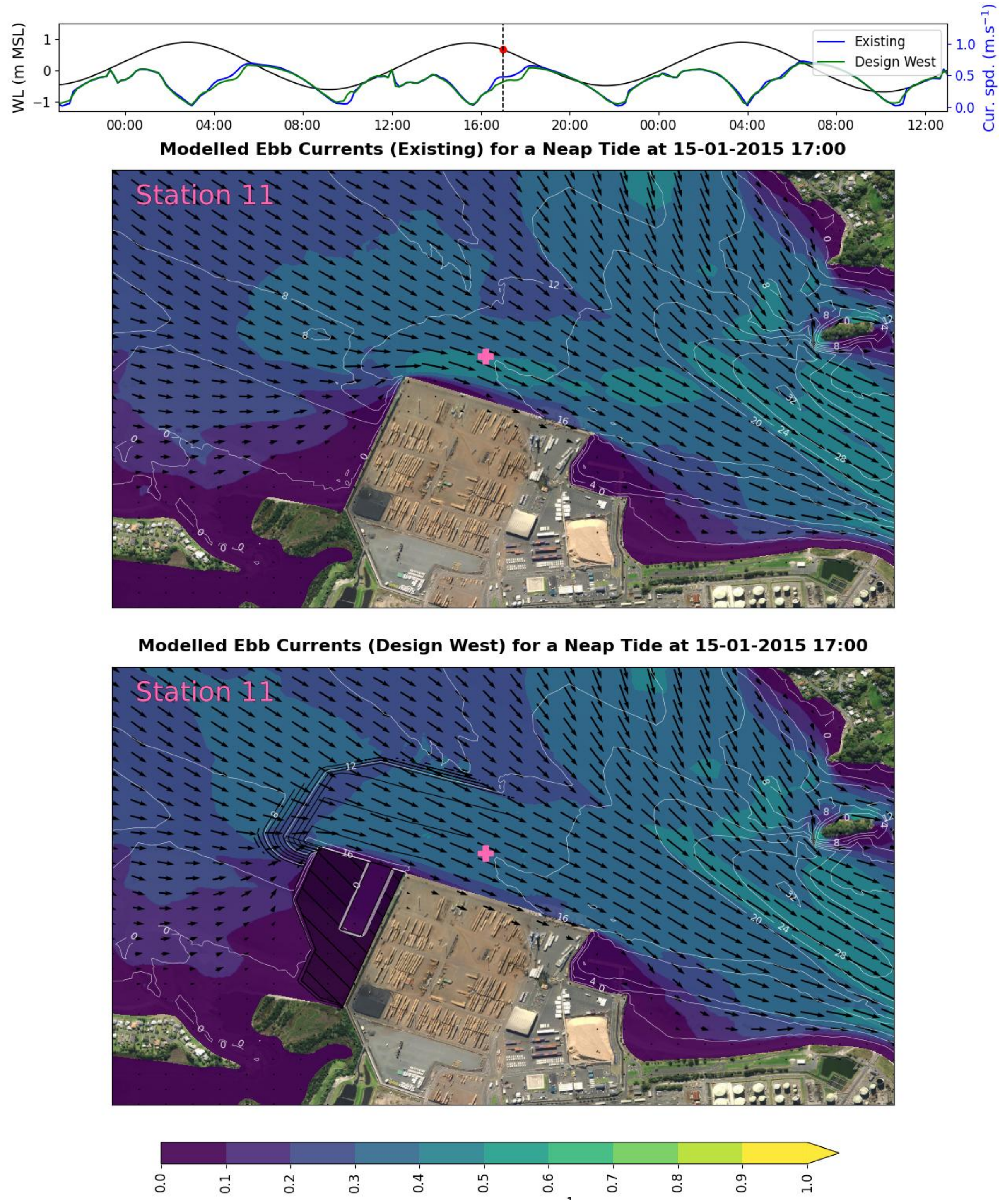

Figure 4-10 Modelled current vectors for the Existing (top) and Design West layout (bottom) during the peak of an ebb neap tide and the bathymetry and depth contours used in each simulation. Black design lines display the proposed reclamation and dredging.

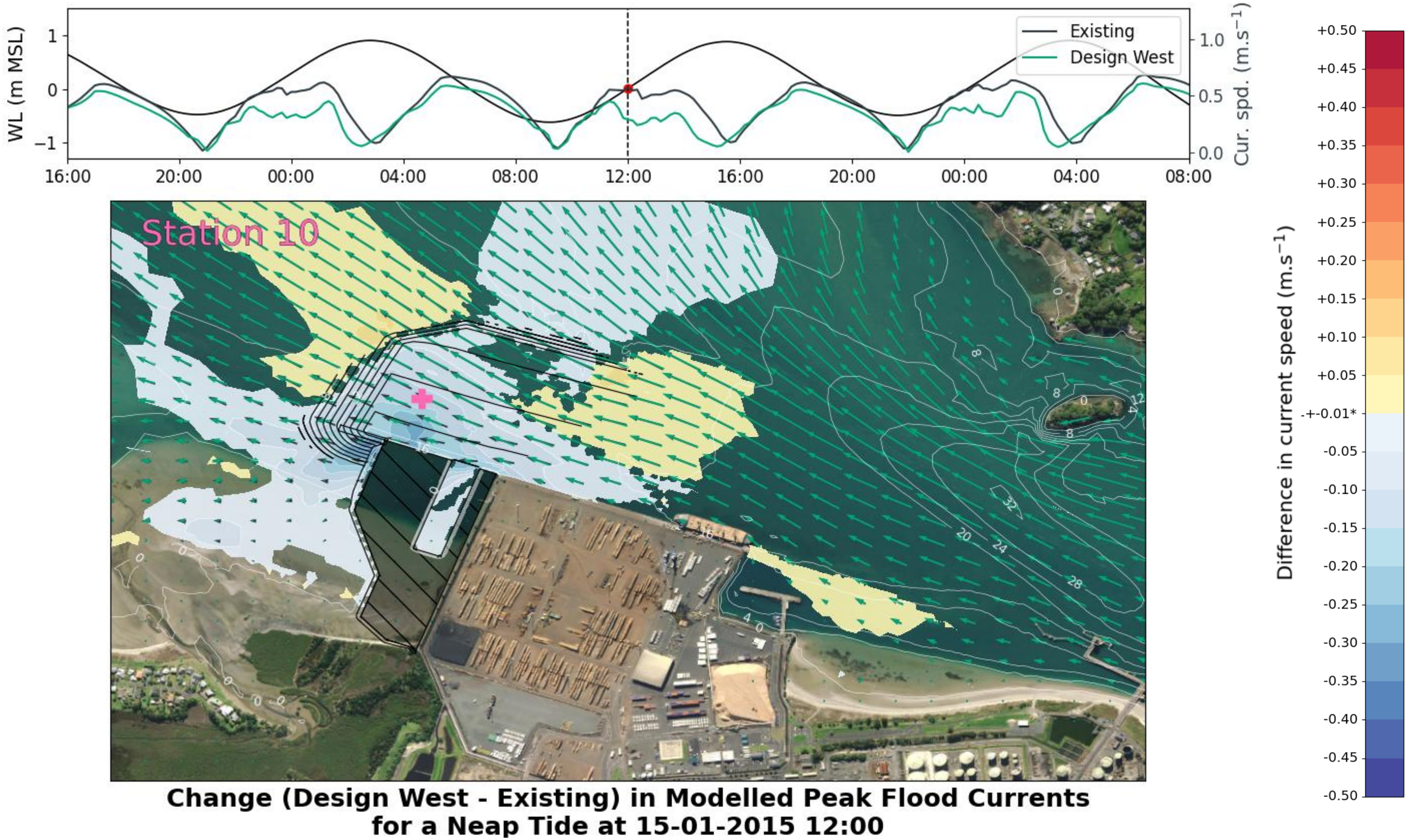

Figure 4-11 Modelled current vectors for the Existing and Design West layout and difference in current magnitude during the peak of a flood neap tide. Note potential changes less than 0.01 $m.s^{-1}$ are masked as they are within the magnitude of model error and were not considered as a meaningful change.

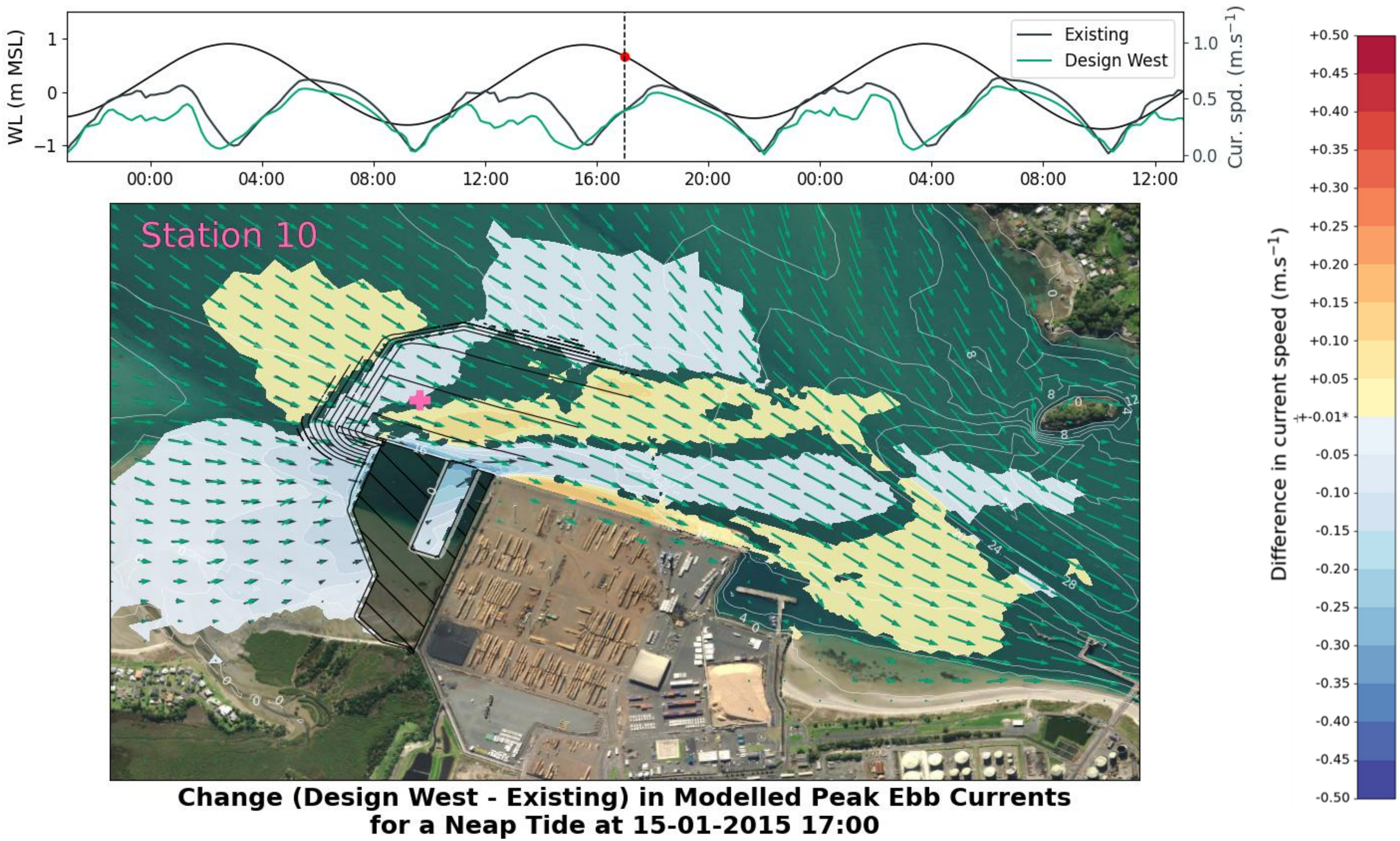

Figure 4-12 Modelled current vectors for the Existing and Design West layout and difference in current magnitude during the peak of an ebb neap tide. Note potential changes less than 0.01 m.s-1 are masked as they are within the magnitude of model error and were not considered as a meaningful change.

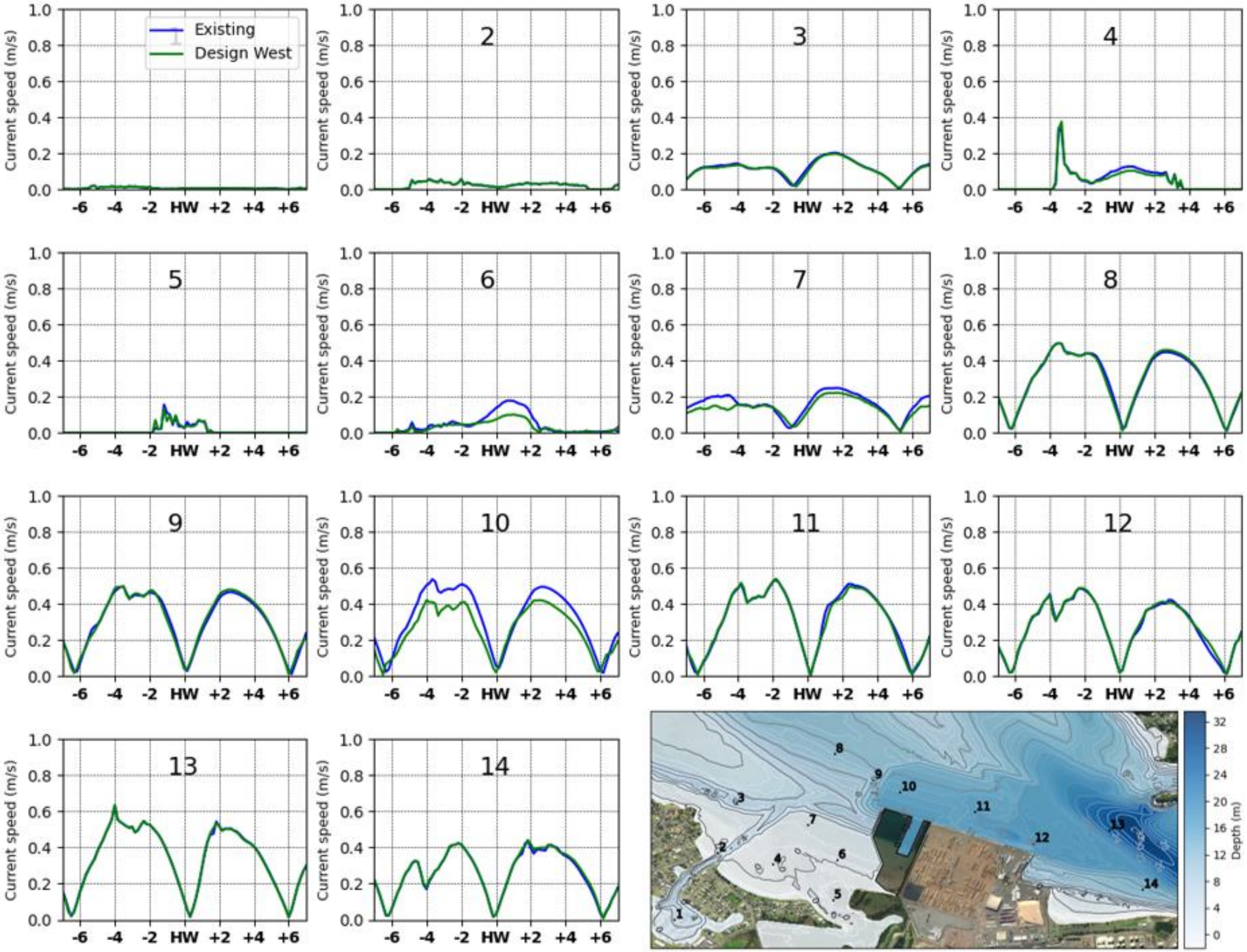

Figure 4-13 Comparisons between modelled current magnitudes for the Existing and Design West layout for 13 hours of a typical neap tidal cycle.

4.2 Effects of Combined Design East and West on hydrodynamics

Comparison of the modelled water levels and currents between the Existing and combined Design East and West simulations over the full simulation period are assessed at selected station output locations. Station output locations and depths are displayed in Figure 3-3 and Figure 3-5. The tidal planes at two stations are displayed in Table 4-1, showing no changes at station 3 in Blacksmith Creek, while a 0.01 m increase in the LAT and 0.01 m decrease in HAT is predicted at station 10 within the dredge footprint.

A statistical analysis of the current speeds at selected stations is provided in Table 4-2. The largest change in current speeds is at station 10 with the 98th percentile current speeds of 1.07 $m.s^{-1}$ and 0.87 $m.s^{-1}$ for the Existing and Design East and West simulations respectively. The percentage difference in mean current speeds is a 30.7% reduction due to the change of depth between the two simulations from 8.4 m to 17.1 m (MSL). Stations 12 near the berth pocket and station 14 to the east of the proposed reclamation also show a reduction in current speeds with the 98th percentile values reducing from 1.02 $m.s^{-1}$ to 0.87 $m.s^{-1}$ at station 12 and 0.96 $m.s^{-1}$ to 0.80 $m.s^{-1}$ at station 14. There is only a 3.0% increase in mean current speeds at station 3.

Timeseries of the modelled Existing and Design East and West water levels, current speeds and directions for the full simulation period at selected stations are displayed in Figure 4-14, Figure 4-15 and Figure 4-16.

Table 4-3 Tidal planes (m) relative to MSL for Existing and Design East and West simulations derived over 29-day lunar cycle for selected stations.

Parameter	Station 3		Station 10	
	Existing (m)	Design East and West (m)	Existing (m)	Design East and West (m)
HAT (Highest Astronomical Tide)	1.30	1.30	1.30	1.29
MHWS (Mean High Water Springs (M2+S2))	1.03	1.03	1.02	1.02
MHWN (Mean High Water Neaps (M2-S2))	0.77	0.77	0.76	0.76
MSL (Mean Sea Level)	0.00	0.00	0.00	0.00
MLWN (Mean Low Water Neaps (-M2+S2))	-0.77	-0.77	-0.76	-0.76
MLWS (Mean Low Water Springs (-M2-S2))	-1.03	-1.03	-1.02	-1.02
LAT (Lowest Astronomical Tide)	-1.31	-1.31	-1.30	-1.31

Table 4-4 Current speed statistics ($m.s^{-1}$) for Existing and Design East and West simulations derived over 29-day lunar cycle for selected stations.

Station	Simulation	Mean	80th %tile	90th %tile	95th %tile	98th %tile	Max	% diff. in mean
Station 3	Existing	0.16	0.22	0.27	0.31	0.34	0.41	3.0%
	Design East and West	0.17	0.23	0.27	0.30	0.34	0.42	
Station 8	Existing	0.53	0.75	0.84	0.91	0.99	1.08	1.4%
	Design East and West	0.54	0.76	0.86	0.94	1.03	1.12	
Station 10	Existing	0.57	0.80	0.89	0.99	1.07	1.22	-30.7%
	Design East and West	0.39	0.57	0.69	0.78	0.87	0.98	
Station 11	Existing	0.55	0.78	0.92	1.00	1.09	1.25	-15.3%
	Design East and West	0.47	0.70	0.83	0.92	1.03	1.16	
Station 12	Existing	0.49	0.68	0.82	0.93	1.02	1.21	-23.6%
	Design East and West	0.37	0.55	0.66	0.77	0.87	1.10	
Station 13	Existing	0.55	0.78	0.91	1.01	1.16	1.35	0.8%
	Design East and West	0.56	0.78	0.89	0.97	1.05	1.28	
Station 14	Existing	0.45	0.64	0.75	0.85	0.96	1.27	-16.1%
	Design East and West	0.38	0.56	0.65	0.72	0.80	0.99	

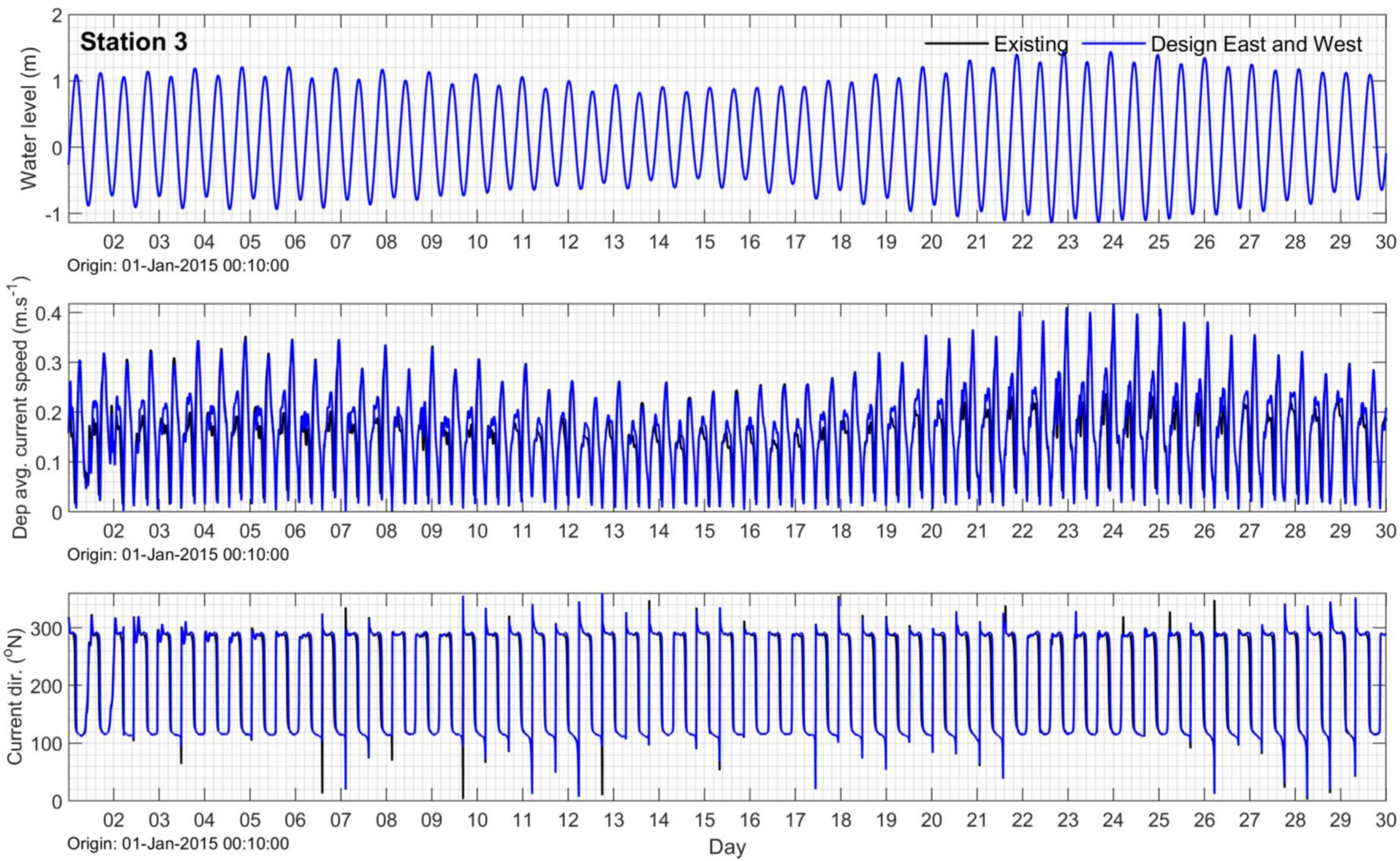

Figure 4-14 Comparison of Existing and Design East and West simulation water levels, current speeds and directions for the full simulation period at station 3.

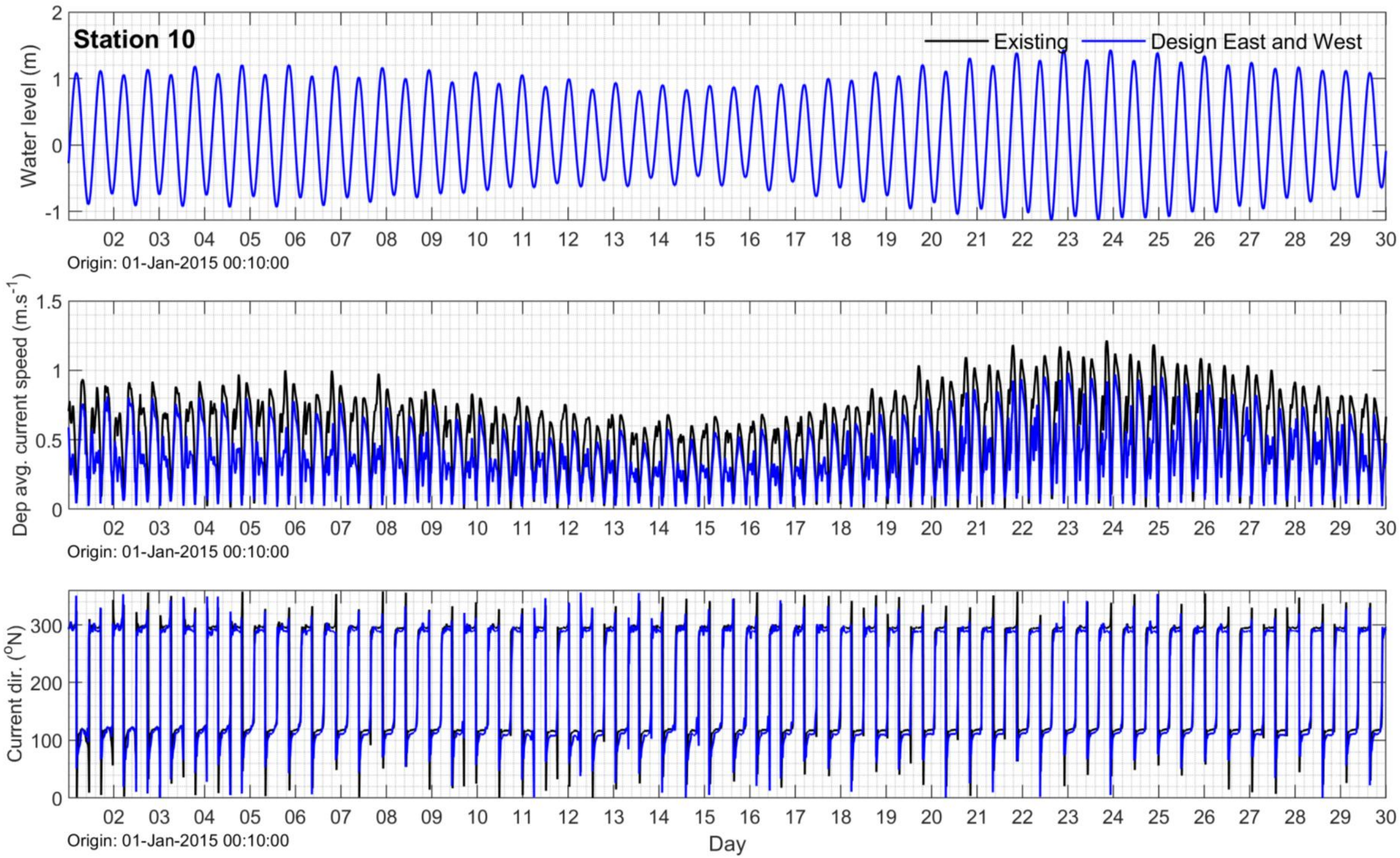

Figure 4-15 Comparison of Existing and Design East and West simulation water levels, current speeds and directions for the full simulation period at station 10.

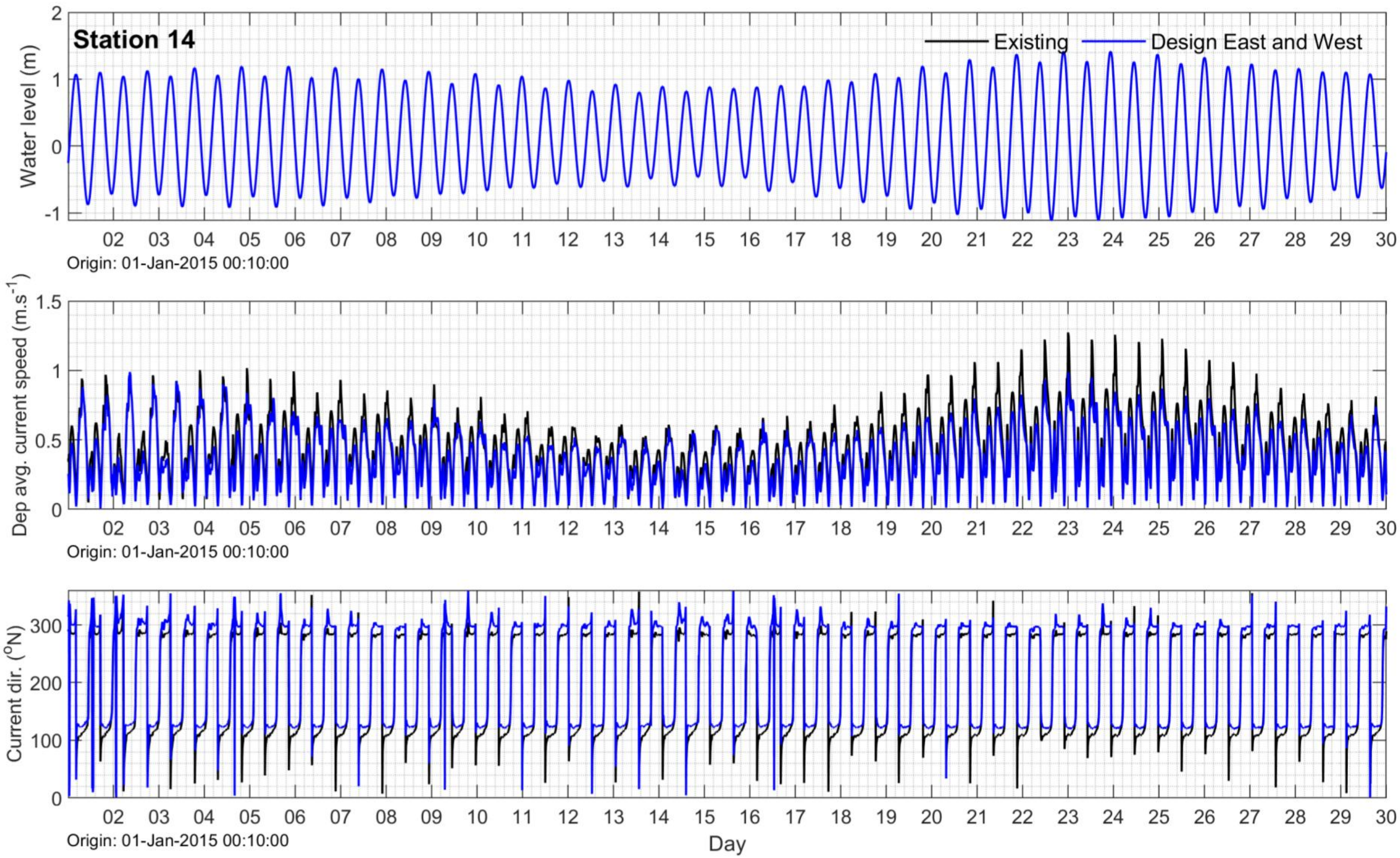

Figure 4-16 Comparison of Existing and Design East and West simulation water levels, current speeds and directions for the full simulation period at station 14.

4.2.1 Spring tidal cycle

Modelled current vectors during a spring tide for the Existing and the proposed Design East and West layout are displayed at peak flood in Figure 4-17 and at peak ebb in Figure 4-18. The predicted changes in current magnitude between the two options (Design East and West-Existing) are presented in Figure 4-19 and Figure 4-20 for the flood and ebb tide respectively. Potential changes less than 0.01 $m.s^{-1}$ are masked as they are within the magnitude of model error and were not considered as a meaningful change.

During peak flood and ebb tide conditions, reductions in current speed are predicted to be less than 0.4 $m{\cdot}s^{-1}$ across the majority of the study area, with localised reductions of up to 0.7 $m{\cdot}s^{-1}$. Decreases in current speeds are observed within the following areas:

- A reduction at the western edge of the dredge footprint. Current speeds decreased in this area due to the increase in depth between the two simulations. The change in depth varies across the footprint but is 8.4 m to 17.1 m MSL at station 10.
- A reduction in current speed of approximately 0.5–0.6 $m{\cdot}s^{-1}$ is predicted along the eastern edge of the proposed reclamation, where flood tide flows are diverted further into the main channel around the reclamation, and ebb tide flows are sheltered within the lee of the reclamation;
- A reduction of 0.3 $m.s^{-1}$ to the west of the western reclamation on an ebb tide;
- During flood tide conditions, a decrease in current speed of less than 0.2 $m{\cdot}s^{-1}$ is predicted within the northern channel inside the harbour entrance, opposite the port. This reduction is attributed to the deepening of the dredged footprint adjacent to the reclamation to 19.6 m MSL, which directs a greater proportion of the tidal prism alongside the port rather than through the northern flood channel; and
- During ebb tide conditions, a reduction in current speed of less than 0.2 $m{\cdot}s^{-1}$ is predicted in the vicinity of Blacksmith Creek and within the lee of the western reclamation.

Modelled results also show a slight increase in current speeds in some areas during peak flood and ebb tides. The predicted increase in current speeds during both flood and ebb tide conditions is generally less than 0.2 $m{\cdot}s^{-1}$ across the majority of the study area, with localised increases of up to 0.3 $m{\cdot}s^{-1}$. Increased in current speeds are observed within the following areas:

- An increase in current speed of less than 0.2 $m{\cdot}s^{-1}$ is predicted in front of the reclamation area on the eastern side of the dredge footprint during flood tide conditions and less than less than 0.3 $m{\cdot}s^{-1}$ during ebb tidal conditions;

- To the west of the dredge footprint, current speed increases are also predicted to remain below 0.2 $m \cdot s^{-1}$;
- The most significant increases in current speed occur alongside the existing berths, with changes of up to 0.4 $m \cdot s^{-1}$; and
- During flood tide conditions, negligible increases in current speed (<0.2 $m \cdot s^{-1}$) are predicted in the vicinity of Blacksmith Creek.

Further, comparisons of current magnitudes for a spring tide over 13 hours at 14 locations in the vicinity of the port are shown in Figure 4-21. In terms of magnitudes, the potential changes within Blacksmith creek environs can be determined at stations 1-7. Stations 1-5 show less than 0.05 $m.s^{-1}$ of change during both a flood (increased speeds) and ebb tide (reduced speeds). As in the analysis of the Design West, at station 6, which is upstream of the shipyard/reclamation, there is a reduction in current speeds of around 0.2 $m.s^{-1}$ after high water, which is in keeping with the differences displayed in Figure 4-20 during an ebb tide. At station 7 there is an increase in current speed of 0.2 $m.s^{-1}$ before high water on a flood tide.

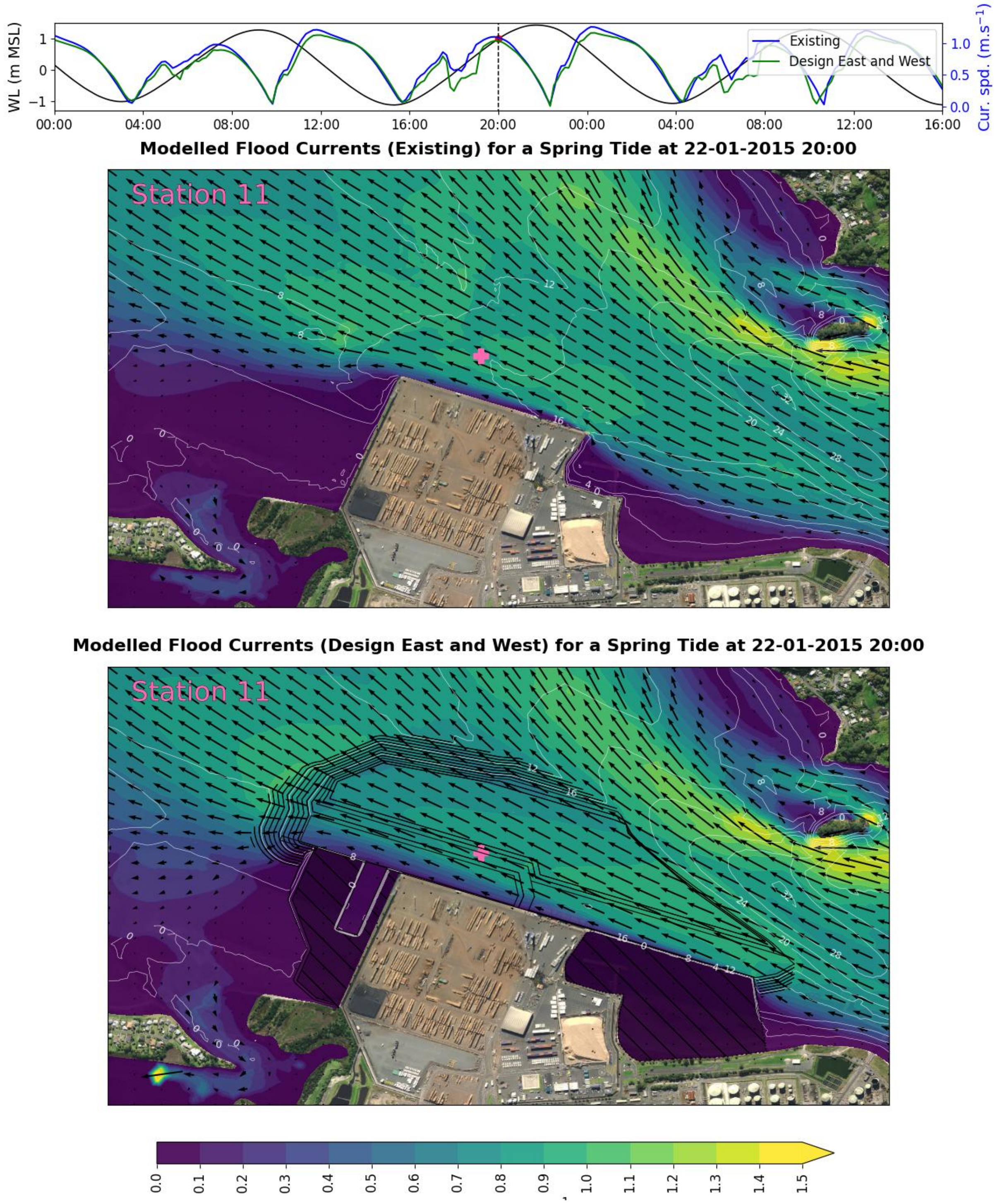

Figure 4-17 Modelled current vectors for the Existing (top) and Design East and West layout (bottom) during the peak of a flood spring tide and the bathymetry and depth contours used in each simulation. Black design lines display the proposed reclamation and dredging.

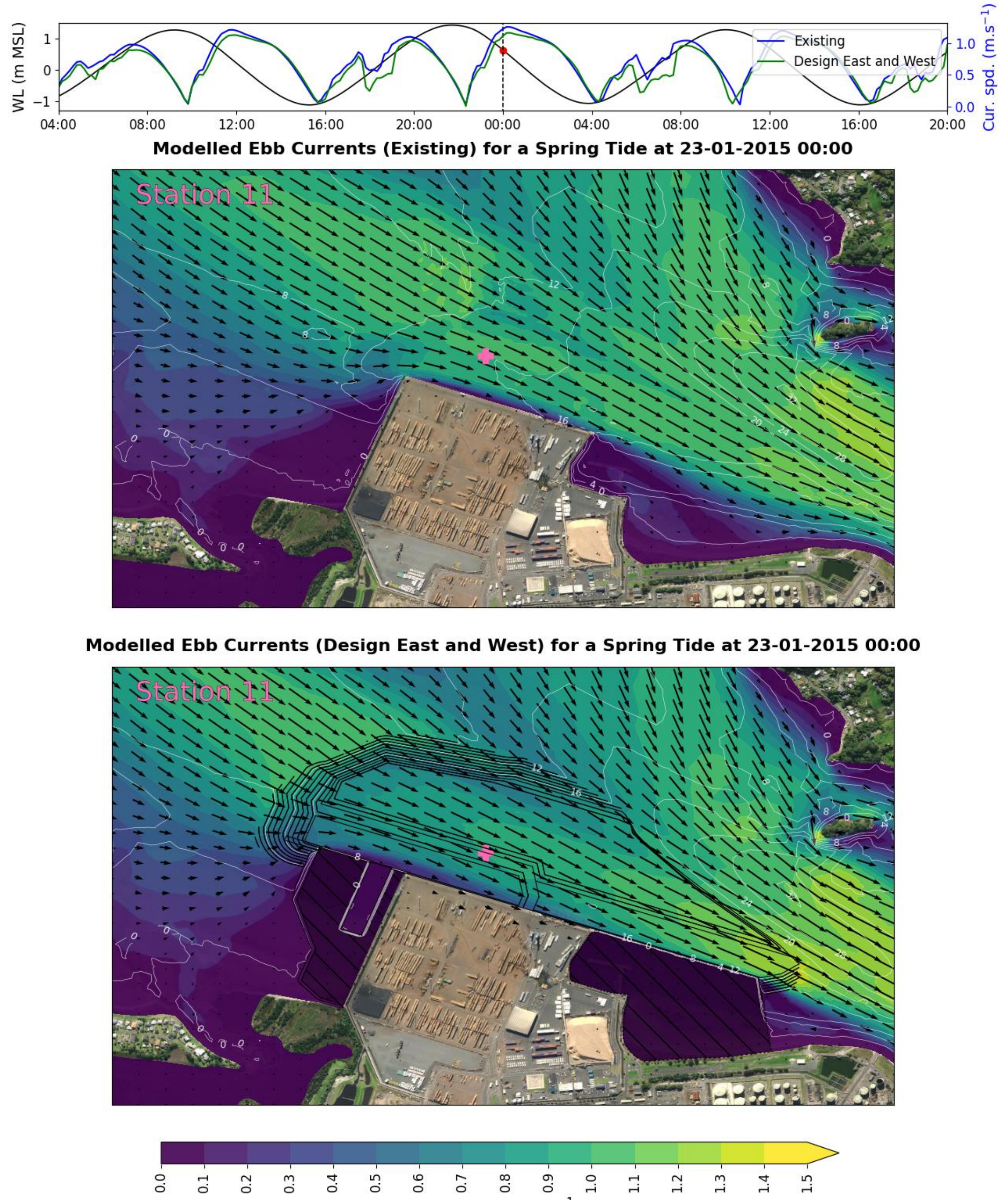

Figure 4-18 Modelled current vectors for the Existing (top) and Design East and West layout (bottom) during the peak of an ebb spring tide and the bathymetry and depth contours used in each simulation. Black design lines display the proposed reclamation and dredging.

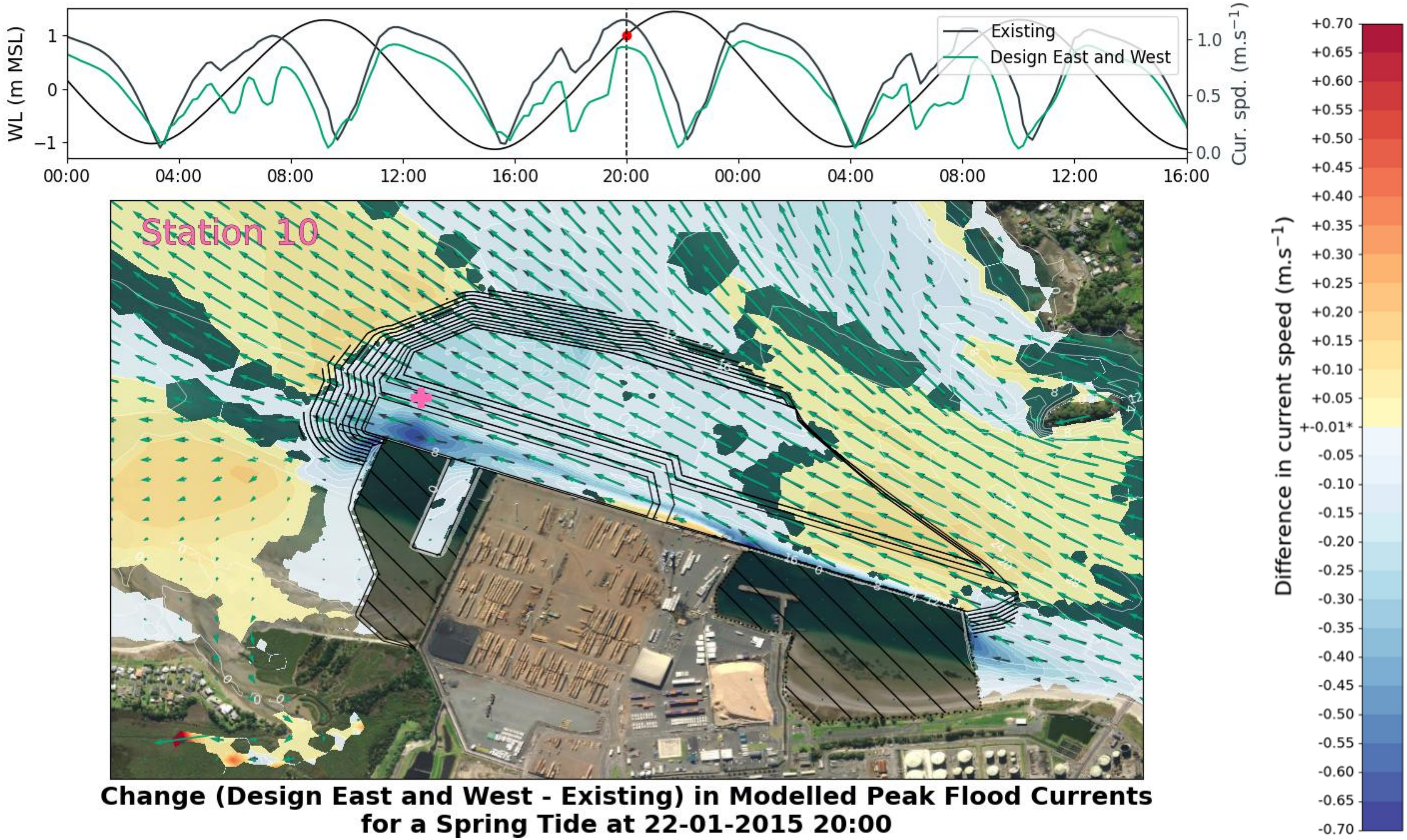

Figure 4-19 Modelled current vectors for the Existing and Design East and West layout and difference in current magnitude during the peak of a flood spring tide. Note potential changes less than 0.01 m.s^{-1} are masked as they are within the magnitude of model error and were not considered as a meaningful change.

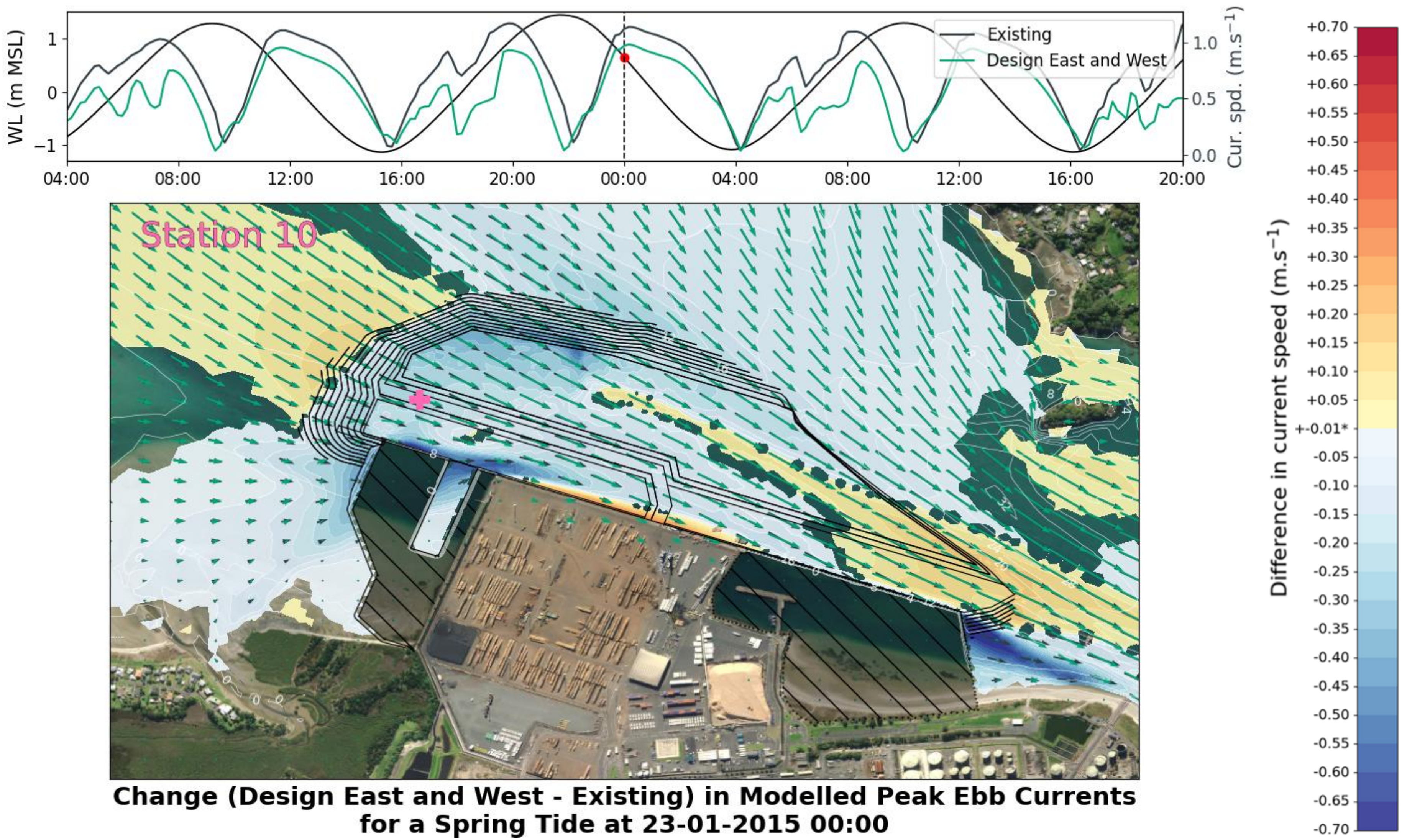

Figure 4-20 Modelled current vectors for the Existing and Design East and West layout and difference in current magnitude during the peak of an ebb spring tide. Note potential changes less than 0.01 m.s^{-1} are masked as they are within the magnitude of model error and were not considered as a meaningful change.

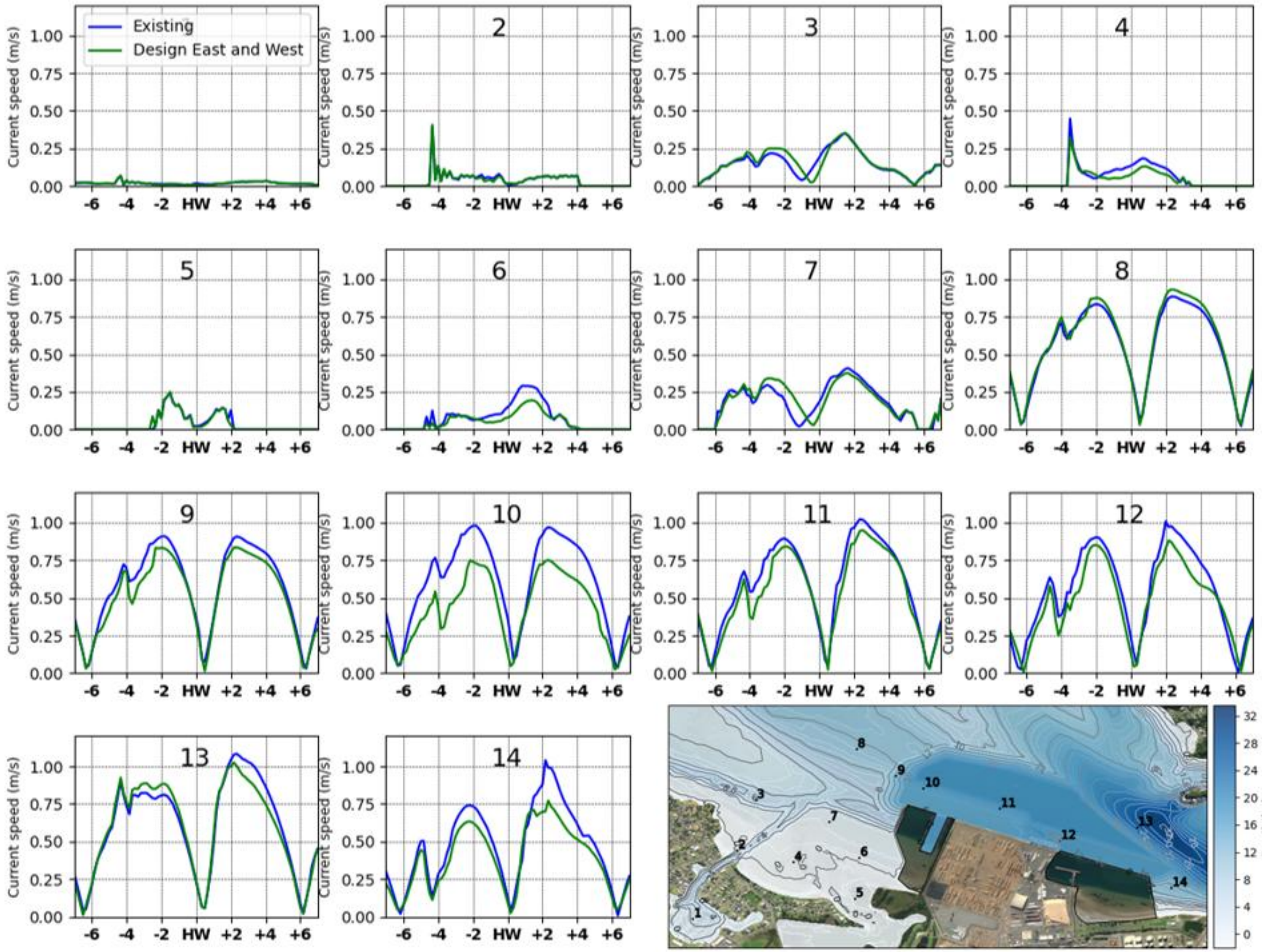

Figure 4-21 Comparisons between modelled current magnitudes for the Existing and Design East and West layout for 13 hours of a typical spring tidal cycle.

4.2.2 Neap tidal cycle

Modelled current vectors during peak flood neap tide for the Existing and Design East and West layout are provided in Figure 4-22 and at peak ebb in Figure 4-23. The predicted change in current magnitude between the two options (Design East and West-Existing) are presented in Figure 4-24 and Figure 4-25 for the flood and ebb tide respectively. In terms of magnitude, the current speed near the project site is about 0.5-0.6 $m.s^{-1}$ during a neap tide, which is approximately half the speed observed during spring tidal flows.

Similar distributions are seen, with the reduction occurring at the western edge of the dredge footprint for both a flood and ebb tide, and a slight reduction in the lee of both the west and east reclamations during an ebb tide. A potential increase in current speeds is also shown to the west of the dredge footprint during flood tide conditions and alongside the existing berths during ebb tide conditions (see Figure 4-24 and Figure 4-25).

Further, comparisons of current magnitudes for a neap tide over 13 hours at 14 locations in the vicinity of the port are shown in Figure 4-26.

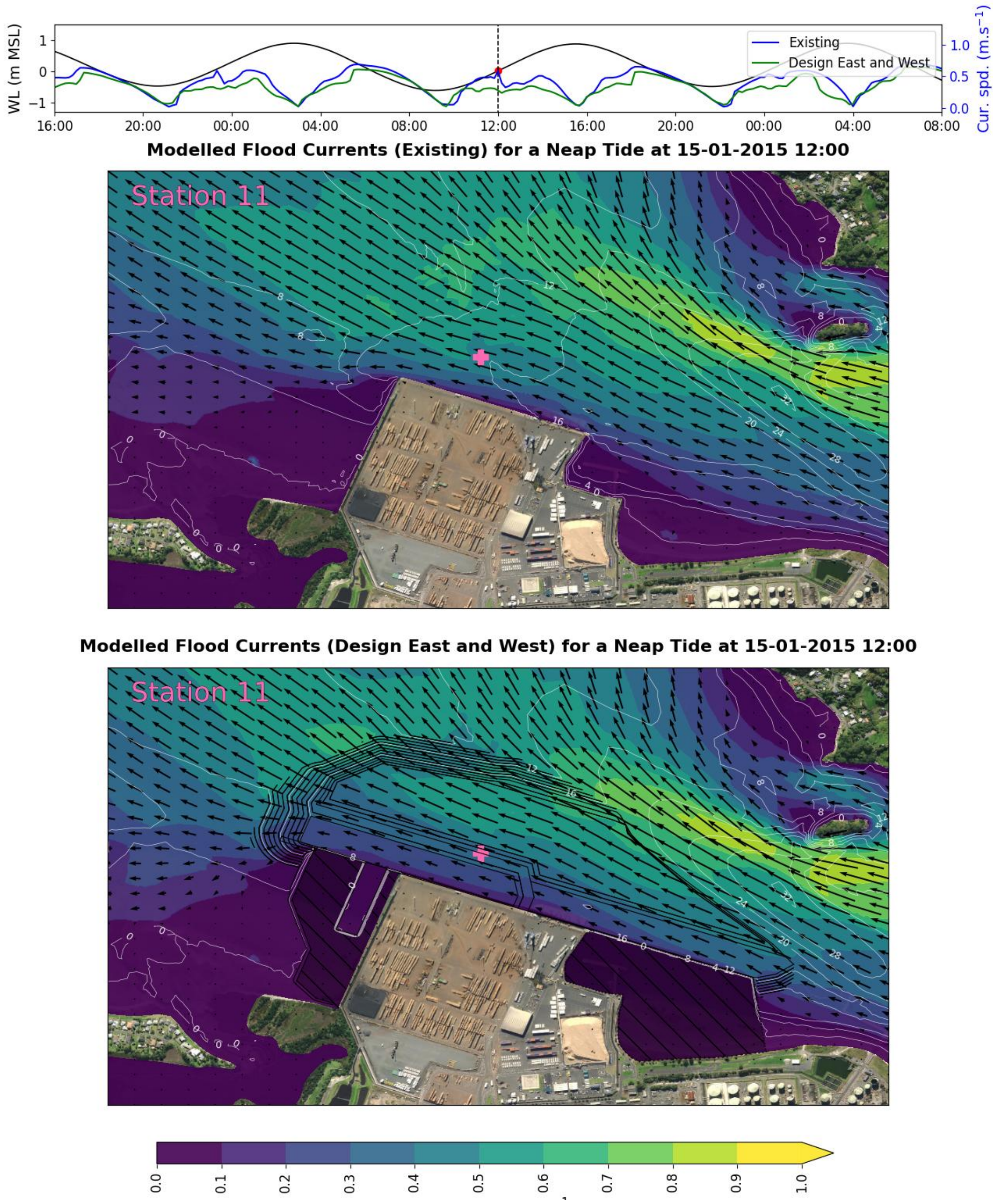

Figure 4-22 Modelled current vectors for the Existing (top) and Design East and West layout (bottom) during the peak of a flood neap tide and the bathymetry and depth contours used in each simulation. Black design lines display the proposed reclamation and dredging.

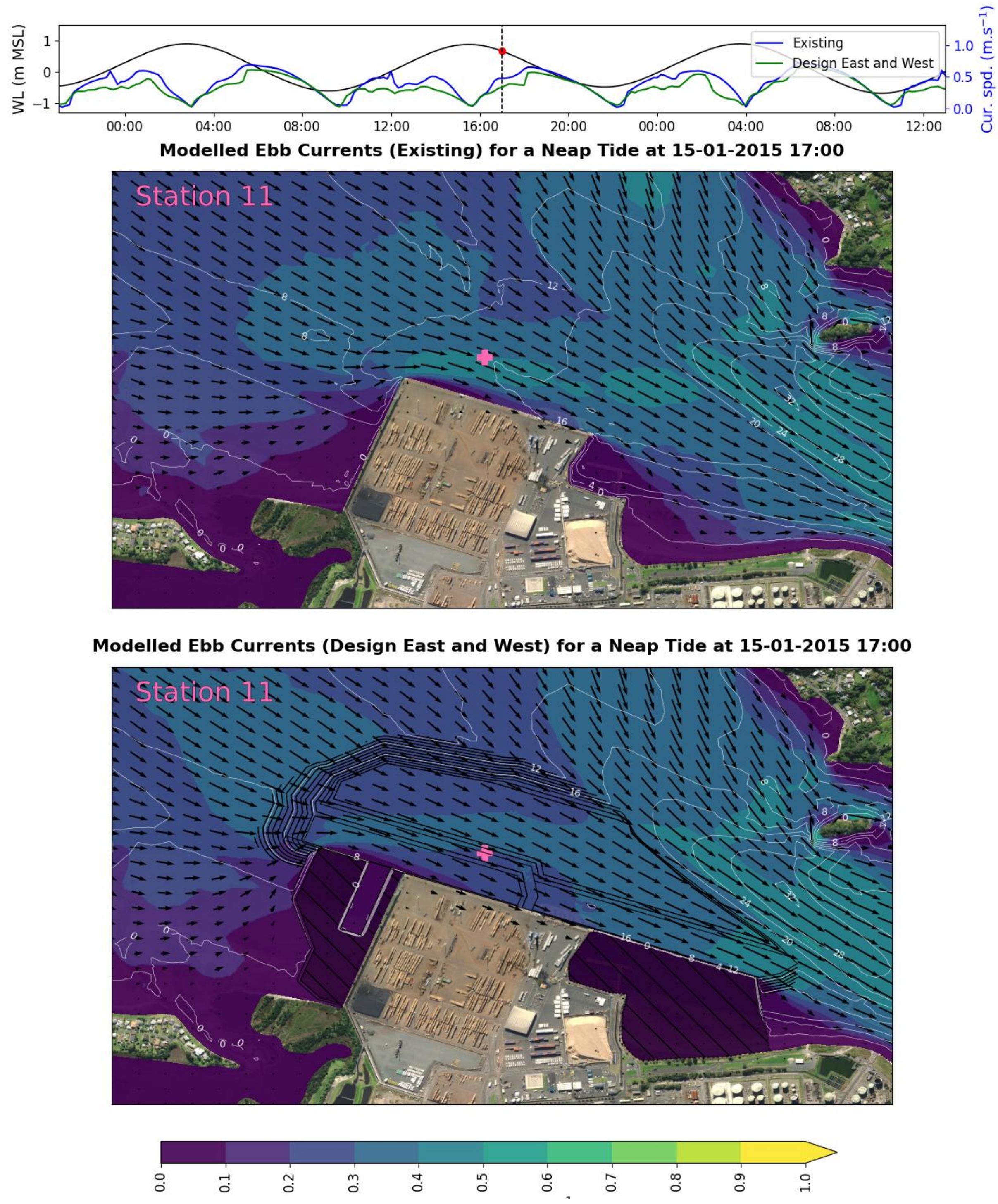

Figure 4-23 Modelled current vectors for the Existing (top) and Design East and West layout (bottom) during the peak of an ebb neap tide and the bathymetry and depth contours used in each simulation. Black design lines display the proposed reclamation and dredging.

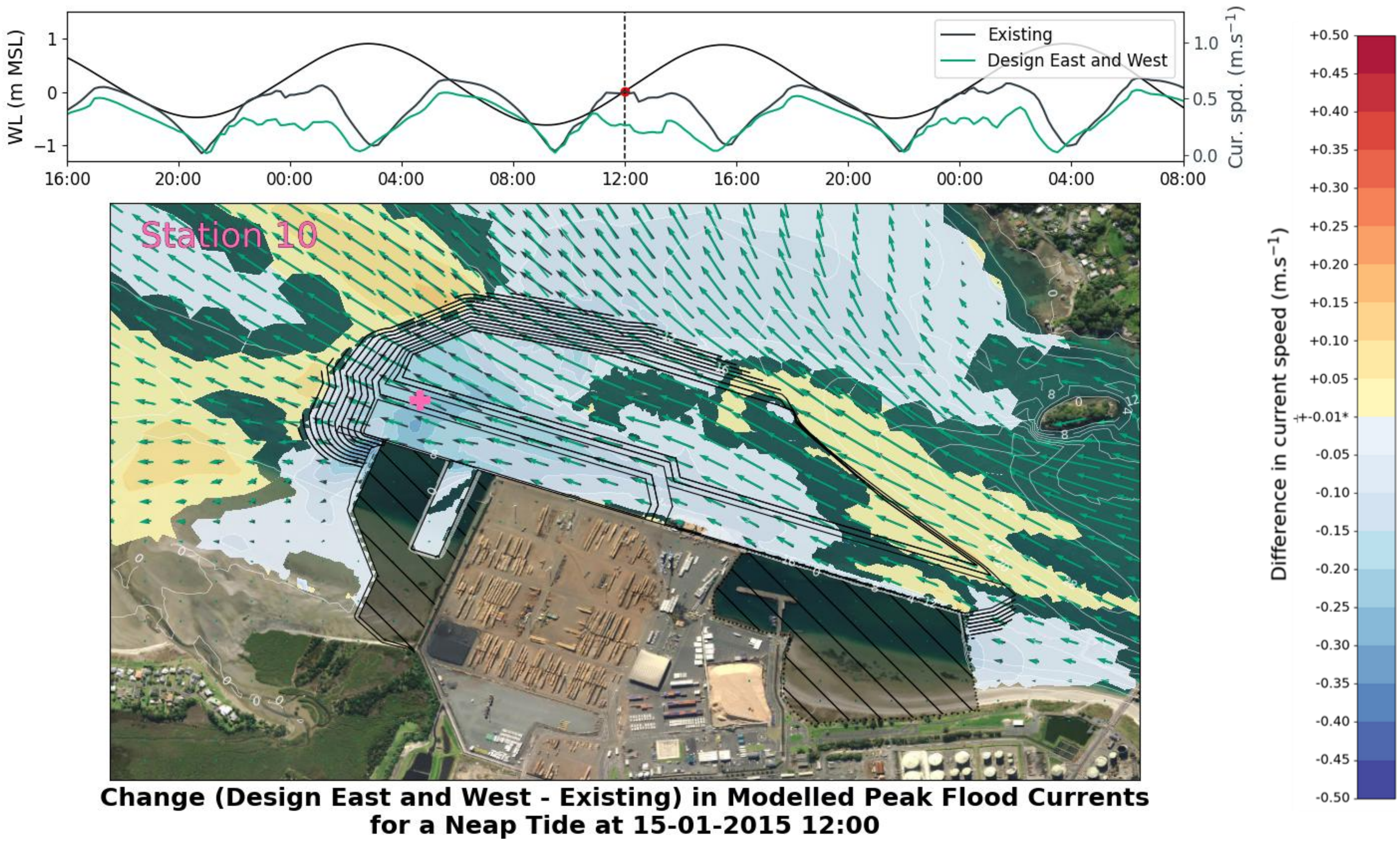

Figure 4-24 Modelled current vectors for the Existing and Design East and West layout and difference in current magnitude during the peak of a flood neap tide. Note potential changes less than 0.01 m.s^{-1} are masked as they are within the magnitude of model error and were not considered as a meaningful change.

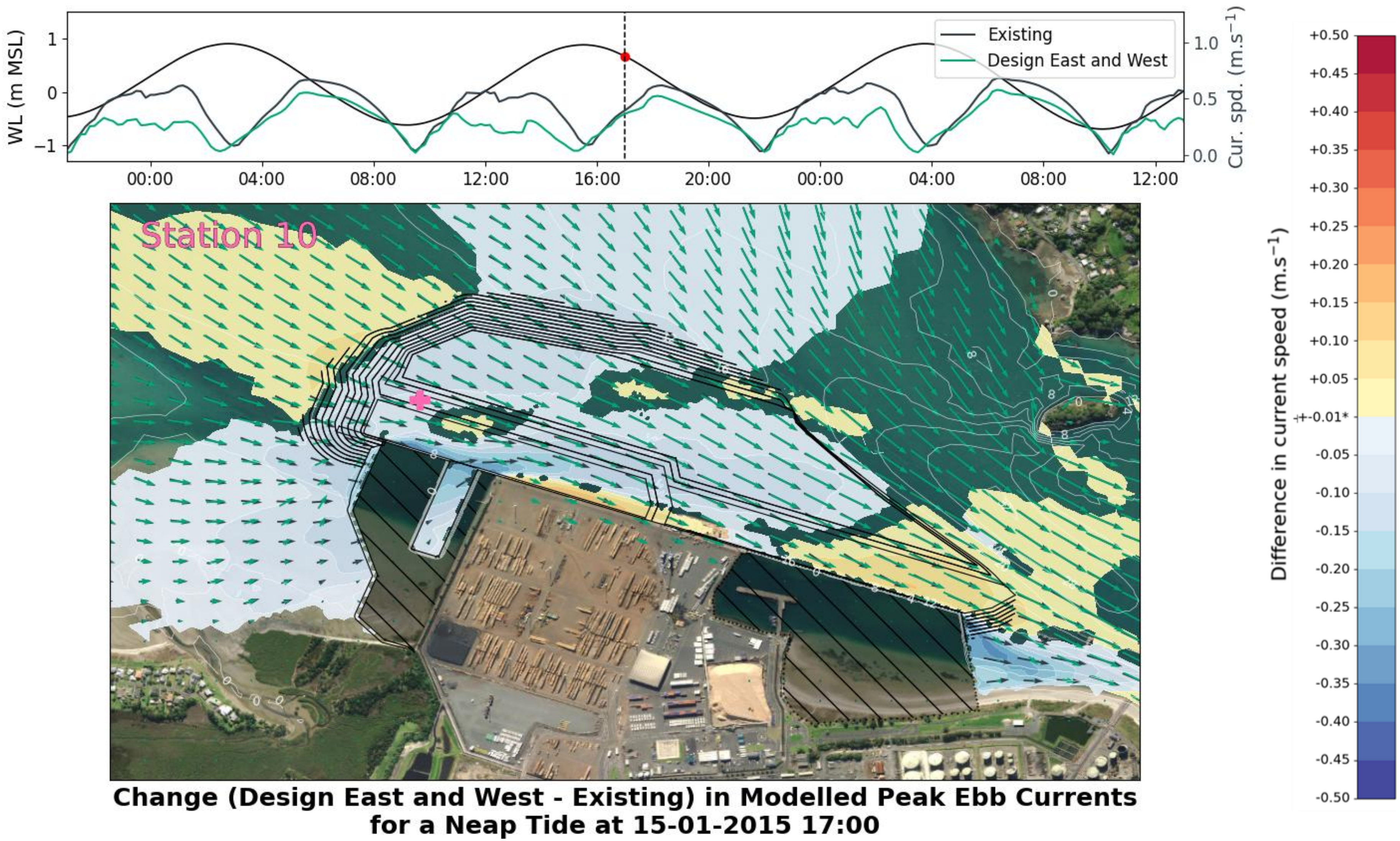

Figure 4-25 Modelled current vectors for the Existing and Design East and West layout and difference in current magnitude during the peak of an ebb neap tide. Note potential changes less than 0.01 m.s^{-1} are masked as they are within the magnitude of model error and were not considered as a meaningful change.

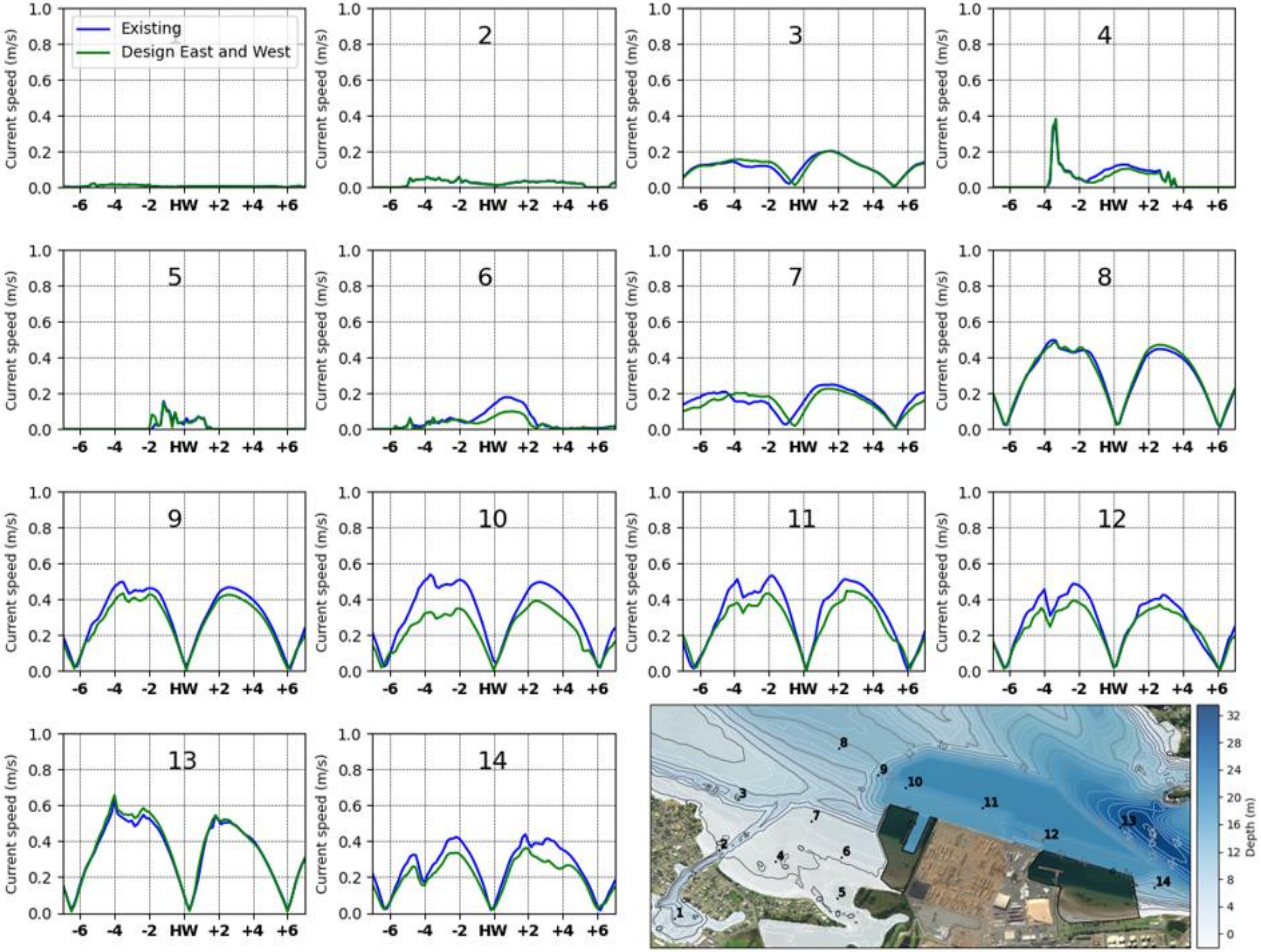

Figure 4-26 Comparisons between modelled current magnitudes for the Existing and Design East and West layout for 13 hours of a typical neap tidal cycle.

5.Summary

In this study, hydrodynamic modelling was undertaken for both Existing and the two proposed designs (Design West, Design East and West) based on 3D SCHISM modelling framework. Results showed that changes in the current field are confined to the region where the dredging and reclamation works will be undertaken which included the following.

Design West

In comparison with the Existing simulations, current speeds under the proposed Design West are expected to decrease within the dredge footprint and in the lee of the western shipyard/reclamation area. Conversely, localised increases in current speeds are anticipated to the west of the dredge footprint and alongside the existing berths.

The proposed Design West layout has only a minor influence on the nearshore current field surrounding Blacksmith Creek during spring tide conditions, with increases of less than 0.1 $m.s^{-1}$ on the flood tide and decreases of approximately 0.2 $m.s^{-1}$ on the ebb tide. The spatial extent of these changes around Blacksmith Creek is smaller than those predicted under the Design East and West scenarios.

The modest reduction in current velocities within the dredge footprint may result in a localised increase in sedimentation potential, particularly during ebb tide conditions, when elevated current speeds immediately upstream of the dredge area may enhance sediment mobility and subsequent deposition within the footprint.

Design East and West

In comparison with the Existing simulations, current speeds under the proposed Design East and West scenarios are expected to decrease at the western edge of the dredge footprint, at the eastern extent of the eastern reclamation area, and within the lee of the western shipyard/reclamation area. Conversely, localised increases in current speeds are predicted in front of the eastern reclamation area within the eastern side of the dredge footprint, to the west of the dredge footprint, and alongside the existing berths.

The proposed Design East and West layouts have only a minor influence on the nearshore current field surrounding Blacksmith Creek during spring tide conditions, with increases of less than 0.2 $m.s^{-1}$ on the flood tide and decreases of approximately 0.2 $m.s^{-1}$ on the ebb tide. Minor reductions in current speed are also predicted within the northern channel inside the harbour entrance opposite the port; however, these are limited to less than 0.2 $m.s^{-1}$.

The localised reduction in current velocities at the eastern extent of the eastern reclamation area indicates a potential increase in sedimentation. Similarly, the western edge of the dredge footprint may be susceptible to increased sediment deposition, particularly during ebb tide conditions, where elevated upstream current speeds may enhance sediment mobility, promoting subsequent deposition within the dredge footprint.

6.References

Deltares, 2018a. User Manual Delft3D-FLOW, Version: 3.15. ed. Deltares.

Deltares, 2018b. User Manual Delft3D-WAVE, Version: 3.05. ed. Deltares.

Haidvogel, D.B, Arango, H.G., Budgell, W.P., Cornuelle, B.D., Curchitser, E., Di Lorenzo, E., Fennel, K., Geyer, W.R., Hermann, A.J., Lanerolle, L., Levin, J., McWilliams, J.C., Miller, A.J., Moore, A.M., Powell, T.M., Shchepetkin, A.F., Sherwood, C.R., Signell, R.P., Warner, J.C., Wilkin, J., 2008. Ocean forecasting in terrain-following coordinates: Formulation and skill assessment of the Regional Ocean Modeling System. Journal of Computational Physics 227, 3595–3624.

Holthuijsen, L.H., Booij, N., Ris, R.C., Haagsma, I.J., Kieftenburg, A.T.M.M., Kriezi, E.E., Zijlema, M., van der Westhuysen, A.J., 2007. SWAN cycle III version 40.51, Technical Documentation. Delft, 2600 GA Delft The Netherlands.

Liu, Z., Wang, H., Zhang, Y.J., Magnusson, L., Loftis, J.D., Forrest, D., 2020. Cross-scale modeling of storm surge, tide, and inundation in Mid-Atlantic Bight and New York City during Hurricane Sandy, 2012. Estuarine, Coastal and Shelf Science 233, 106544. https://doi.org/https://doi.org/10.1016/j.ecss.2019.106544

Lopes, V., Silva, P.A., Bertin, X., Fortunato, A.B., Oliveira, A., 2009. Impact of a Dredged Sandpit on Tidal and Wave Hydrodynamics. Journal of Coastal Research 529–533.

Mendes, D.S., Fortunato, A.B., Pires-Silva, A.A., 2016. Assessment of three dredging plans for a wave-dominated inlet. Proceedings of the Institution of Civil Engineers - Maritime Engineering 169, 64–75. https://doi.org/10.1680/jmaen.2015.7

MetOcean Solutions, 2023. Hydrodynamic Modelling Additional Output Locations - Effects of Proposed Reclamation and Dredging Layout on Hydrodynamics (Report prepared for Northport No. Report P0519-13).

MetOcean Solutions, 2022a. Hydrodynamic Modelling Update - Effects of Proposed Reclamation and Dredging Layout on Hydrodynamics (Report prepared for Northport No. Report P0519-10).

MetOcean Solutions, 2022b. Morphodynamic Modelling for the Northport Environment. Modelling Update . Predicted morphological response to proposed eastern land reclamation (Report prepared for Northport No. Report P0519-11).

MetOcean Solutions, 2021a. Hydrodynamic Modelling - Effect of Proposed Reclamation Layouts on Hydrodynamics (Report prepared for Northport No. Report P0519-01).

MetOcean Solutions, 2021b. Morphodynamic Modelling for the Northport Environment. Modelling Update . Predicted morphological response to proposed capital dredging and land reclamation (Report prepared for Northport No. Report P0519-02).

MetOcean Solutions, 2021c. Dredge Plume Modelling . Dredging sediment plume dispersion over existing and proposed port configurations (Report prepared for Northport No. Report P0519-03).

MetOcean Solutions, 2019. Waste Water Dispersion Modelling (Report prepared for Refining New Zealand (RNZ) No. Report P0460).

MetOcean Solutions, 2018a. Morphodynamic Evolution Modelling for the Northport Environment - Predicted morphological response to proposed capital dredging and land reclamation (Report prepared for Northport No. Report P0367–03).

MetOcean Solutions, 2018b. Morphodynamic Evolution Modelling for the Northport Environment - Morphological model calibration (Report prepared for Northport No. Report P0367–01 Rev B).

MetOcean Solutions, 2018c. Morphodynamic Evolution Modelling for the Northport Environment - Five year morphological prediction of the swinging basin morphological response (Report prepared for Northport No. Report P0367–05).

MetOcean Solutions, 2018d. Northport Dredging Project - Dredging Plume Modelling (Report prepared for Northport No. Report P0367–01).

MetOcean Solutions, 2018e. Dredging Plumes for NorthPort Environment (Report prepared for Northport No. Report P0367-04).

MetOcean Solutions, 2018f. Hydrodynamic Modelling - Methodology, Validation and Simulations (Report prepared for Northport No. Report P0367-02).

MetOcean Solutions, 2016. Characterisation of the physical environment at the Whangarei Harbour entrance and establishment of numerical models of wave, current and sediment dynamics (Report prepared for Refining New Zealand No. Crude Freight Shipping Project Whangarei Harbour).

Paulik, R., Stephens, S., 2023. Mapping New Zealand's exposure to coastal flooding and sea-level rise (NIWA internal report No. NIWA internal report).

Saha, S., Moorthi, S., Pan, H.-L., Wu, X., Wang, Jiande, Nadiga, S., Tripp, P., Kistler, R., Woollen, J., Behringer, D., Liu, H., Stokes, D., Grumbine, R., Gayno, G., Wang, Jun, Hou, Y.-T., Chuang, H.-Y., Juang, H.-M.H., Sela, J., Iredell, M., Treadon, R., Kleist, D., Van Delst, P., Keyser, D., Derber, J., Ek, M., Meng, J., Wei, H., Yang, R., Lord, S., Van Den Dool, H., Kumar, A., Wang, W., Long, C., Chelliah, M., Xue, Y., Huang, B., Schemm, J.-K., Ebisuzaki, W., Lin, R., Xie, P., Chen, M., Zhou, S., Higgins, W., Zou, C.-Z., Liu, Q., Chen, Y., Han, Y., Cucurull, L., Reynolds, R.W., Rutledge, G., Goldberg, M., 2010. The NCEP Climate Forecast System Reanalysis. Bull. Amer. Meteor. Soc. 91, 1015–1057. https://doi.org/10.1175/2010BAMS3001.1

Song, Y.T., Hou, T.Y., 2006. Parametric vertical coordinate formulation for multiscale, Boussinesq, and non-Boussinesq ocean modeling. Ocean Modelling 11, 298–332. https://doi.org/https://doi.org/10.1016/j.ocemod.2005.01.001

Ye, F., Zhang, Y.J., Friedrichs, M.A.M., Wang, H.V., Irby, I.D., Shen, J., Wang, Z., 2016. A 3D, cross-scale, baroclinic model with implicit vertical transport for the Upper Chesapeake Bay and its tributaries. Ocean Modelling 107, 82–96. https://doi.org/https://doi.org/10.1016/j.ocemod.2016.10.004

Ye, F., Zhang, Y.J., Wang, H.V., Friedrichs, M.A.M., Irby, I.D., Alteljevich, E., Valle-Levinson, A., Wang, Z., Huang, H., Shen, J., Du, J., 2018a. A 3D unstructured-grid model for

Chesapeake Bay: Importance of bathymetry. Ocean Modelling 127, 16–39. https://doi.org/https://doi.org/10.1016/j.ocemod.2018.05.002

Ye, F., Zhang, Y.J., Wang, H.V., Huang, H., Wang, Z., Liu, Z., Li, X., 2018b. Cross-Scale Baroclinic Simulation of the Effect of Channel Dredging in an Estuarine Setting. Water 10. https://doi.org/10.3390/w10020163

Zhang, Y., Ateljevich, E., Yu, H.-C., Wu, C., Yu, J., 2014. A new vertical coordinate system for a 3D unstructured-grid model. Ocean Modelling 85. https://doi.org/10.1016/j.ocemod.2014.10.003

Zhang, Y.J., Gerdts, N., Ateljevich, E., Nam, K., 2020. Simulating vegetation effects on flows in 3D using an unstructured grid model: model development and validation. Ocean Dynamics 70, 213–230. https://doi.org/10.1007/s10236-019-01333-8

Zhang, Y.J., Ye, F., Stanev, E.V., Grashorn, S., 2016. Seamless cross-scale modeling with SCHISM. Ocean Modelling 102, 64–81.

Zhang, Y.L., Baptista, A.M., 2008. A semi-implicit Eulerian-Lagrangian finite element model for cross-scale ocean circulation. Ocean Modelling 21, 71–96.